

# **A series of nickel(ii) thiocyanate complexes comprising various molar contents of isonicotinamide and water as ligands or co-crystallized moieties – an experimental and computational study**

Lucija Hok, Robert Vianello, Dubravka Matković-Čalogović, Ljiljana Karanović, Sunčica Roca, Jarosław Jaźwiński, Marina Tašner, Darko Vušak, Marijana Đaković, Zora Popović



**Дигитални репозиторијум Рударско-геолошког факултета Универзитета у Београду**

**[ДР РГФ]**

A series of nickel(ii) thiocyanate complexes comprising various molar contents of isonicotinamide and water as ligands or co-crystallized moieties – an experimental and computational study | Lucija Hok, Robert Vianello, Dubravka Matković-Čalogović, Ljiljana Karanović, Sunčica Roca, Jarosław Jaźwiński, Marina Tašner, Darko Vušak, Marijana Đaković, Zora Popović | CrystEngComm | 2022 | |

10.1039/d2ce00847e

<http://dr.rgf.bg.ac.rs/s/repo/item/0007596>

Дигитални репозиторијум Рударско-геолошког факултета Универзитета у Београду омогућава приступ издањима Факултета и радовима запослених доступним у слободном приступу. - Претрага репозиторијума доступна је на [www.dr.rgf.bg.ac.rs](http://www.dr.rgf.bg.ac.rs)

The Digital repository of The University of Belgrade Faculty of Mining and Geology archives faculty publications available in open access, as well as the employees' publications. - The Repository is available at: [www.dr.rgf.bg.ac.rs](http://www.dr.rgf.bg.ac.rs)



Cite this: *CrystEngComm*, 2022, 24, 6564

## A series of nickel(II) thiocyanate complexes comprising various molar contents of isonicotinamide and water as ligands or co-crystallized moieties – an experimental and computational study†

Lucija Hok, <sup>a</sup> Robert Vianello, <sup>\*a</sup> Dubravka Matković-Čalogović, <sup>b</sup> Ljiljana Karanović, <sup>c</sup> Sunčica Roca, <sup>a</sup> Jarosław Jaźwiński, <sup>d</sup> Marina Tašner,<sup>b</sup> Darko Vušak,<sup>b</sup> Marijana Đaković <sup>b</sup> and Zora Popović <sup>\*b</sup>

Seven complexes,  $[\text{Ni}(\text{NCS})_2(\text{isn})_2(\text{H}_2\text{O})_2] \cdot 2\text{H}_2\text{O}$  (**1**),  $[\text{Ni}(\text{NCS})_2(\text{isn})_2(\text{H}_2\text{O})_2]$  (**2**),  $[\text{Ni}(\text{NCS})_2(\text{isn})_3(\text{H}_2\text{O})] \cdot 2.5\text{H}_2\text{O}$  (**3**),  $[\text{Ni}(\text{NCS})_2(\text{isn})_3(\text{H}_2\text{O})] \cdot 3[\text{Ni}(\text{NCS})_2(\text{isn})_4] \cdot 9\text{H}_2\text{O}$  (**4**),  $[\text{Ni}(\text{NCS})_2(\text{isn})_4] \cdot 3\text{H}_2\text{O}$  (**5**),  $[\text{Ni}(\text{NCS})_2(\text{isn})_4] \cdot 2(\text{isn})$  (**6**) and  $[\text{Ni}(\text{NCS})_2(\text{isn})_4] \cdot 1.25\text{H}_2\text{O}$  (**7**), of Ni(II) thiocyanate with isonicotinamide (isn = pyridine-4-carboxamide) and water as ligands of biological importance were prepared in aqueous solutions through crystal screening by variation of the isonicotinamide concentration. They were characterized by the single-crystal X-ray diffraction method and DFT calculations, while **1–6** were characterized also by NMR and IR spectroscopy and elemental and thermal analyses. In all complexes, the nickel atom is octahedrally coordinated with two thiocyanate N atoms but with different number of isonicotinamide N and water O atoms. The  $R_6^4(12)$  and  $R_6^4(16)$  hexamers were found in **1**,  $R_4^2(8)$  tetramer and  $R_2^2(8)$  dimer in **2**, while very complex hydrogen bonding ring patterns  $R_4^2(8)$ ,  $R_2^2(10)$ ,  $R_4^3(14)$  and  $R_{10}^6(24)$  were observed in **3**. In **4**,  $R_6^4(16)$  and  $R_6^6(20)$  hexamers were formed as well as typical head-to-head amide–amide hydrogen bond  $R_2^2(8)$  dimers in a combination with two  $R_4^3(10)$  tetramers.  $R_4^2(8)$  cyclic water tetramers linked in zigzag hydrogen bonded chains, carboxamide catemer C(4) chains with the  $R_8^6(24)$  ring and two fused rings  $R_3^2(12)$  and  $R_2^2(16)$  were found in **5**. A 2D corrugated sheet network in the (002) planes with a combination of  $R_4^4(16)$ ,  $R_6^4(16)$ ,  $R_6^6(24)$  and  $R_8^6(24)$  rings were formed in **6**. DFT calculations revealed that altered metal complex stoichiometries originate in different ligand affinities towards nickel,  $\text{isn} > \text{SCN}^- > \text{H}_2\text{O}$ . Only neutral complexes were investigated so the nickel:thiocyanate ratio was always 1:2 while the concentration of isonicotinamide strongly influenced the number of coordinated isn ligands. The final 3D crystal structures emerged as a compromise between the nucleation process, reactant ratios, ligand affinities and intermolecular interactions in the crystal packing.

Received 21st June 2022,  
Accepted 14th August 2022

DOI: 10.1039/d2ce00847e

[rsc.li/crystengcomm](http://rsc.li/crystengcomm)

<sup>a</sup> Ruder Bošković Institute, Zagreb, Croatia. E-mail: robert.vianello@irb.hr

<sup>b</sup> Department of Chemistry, Faculty of Science, University of Zagreb, Zagreb, Croatia. E-mail: zpopovic@chem.pmf.hr

<sup>c</sup> Laboratory for Crystallography, Faculty of Mining and Geology, University of Belgrade, Belgrade, Serbia

<sup>d</sup> Institute of Organic Chemistry, Polish Academy of Sciences, Warsaw, Poland

† Electronic supplementary information (ESI) available: Various preparation experiments, structural, thermogravimetric, spectroscopic and computational details for complexes **1–7** (PDF). CCDC 2177868–2177873 contain the supplementary crystallographic data for **1–6** and 2178978 for **7**. For ESI and crystallographic data in CIF or other electronic format see DOI: <https://doi.org/10.1039/d2ce00847e>

## Introduction

The design of supramolecular architectures by the self-assembly of small molecules into more complex ones has become a major research area owing to the recognition of their practical applications.<sup>1–6</sup> Besides pharmaceutical co-crystals that are readily engaged in supramolecular synthons,<sup>7</sup> hydrate co-crystals are omnipresent in crystal engineering of many metal complexes as well. The metal–ligand bond plays a determining role influencing the resultant supramolecular topology. Secondary interactions, such as hydrogen bonding,  $\pi$ – $\pi$  interactions, *etc.*, also have a significant influence in shaping the final architecture. Self-assembly of the coordination frameworks is also highly affected by various

other parameters such as the dynamic nature of the metal–ligand bonds, structural preferences of the metal ions, nature of the ligand ligating topologies, metal–ligand ratios, nature of the counter ions and various experimental conditions (solvent, pH, temperature, crystallization methods). Therefore, it is still a demanding task to predict the final outcome and much work has to be done to improve our understanding of all the factors influencing the resulting supramolecular architecture.

Pyridinecarboxamide ligands have been used as effective tools to organize metal building blocks into extended assemblies by combining their metal-coordinating ability, robust hydrogen-bonding tendency and  $\pi$ – $\pi$  aromatic stacking.<sup>8</sup> In the majority of metal complexes, isonicotinamide (isn) acts as a monodentate ligand through the pyridine nitrogen. Interestingly, four complexes revealed the bridging mode,<sup>9–12</sup> while only two contained the metal-to-ligand bond with deprotonated amide involving a pyridine N-derivative of isonicotinamide.<sup>13,14</sup> Although homoleptic thiocyanate metal complexes have been largely explored, heteroleptic ones, especially those with aromatic amides, have not. In theory, there are thirteen bridging modes for ambidentate thiocyanate, though not all of them have been found.<sup>15</sup> Coordination of thiocyanate to the metal is best understood within Pearson's hard–soft acid–base (HSAB) concept.<sup>16,17</sup> Our earlier work, which we performed under analogous reaction conditions with Cu(II), Zn(II) and Hg(II), gave complexes without water as the third ligand.<sup>18–20</sup> Interestingly, we found other uncommon isonicotinamide supramolecular synthons in Cu(II) coordination compounds directed with nitrate and perchlorate anions.<sup>20</sup> Recently, Neumann *et al.* reported  $[\text{Co}(\text{NCS})_2(\text{isn})_4] \cdot 2(\text{isn}) \cdot \text{EtOH}$  and  $[\text{Co}(\text{NCS})_2(\text{isn})_3(\text{H}_2\text{O})] \cdot 2.5\text{H}_2\text{O}$ ,<sup>21,22</sup> while Wicht *et al.* investigated  $[\text{Ni}(\text{NCS})_2(\text{isn})_4]$  as a host, with water, ethanol (EtOH) and isonicotinamide as guests, and obtained  $[\text{Ni}(\text{NCS})_2(\text{isn})_4] \cdot \text{EtOH} \cdot 0.4\text{H}_2\text{O}$ ,  $[\text{Ni}(\text{NCS})_2(\text{isn})_4] \cdot 2(\text{isn}) \cdot \text{EtOH}$  and  $[\text{Ni}(\text{NCS})_2(\text{isn})_4] \cdot 3\text{H}_2\text{O}$ .<sup>23</sup>

The mentioned strategy of using building blocks to achieve different 3D assemblies is part of our broader project. We have considered picolinamide (pyridine-2-carboxamide, pia), nicotinamide (pyridine-3-carboxamide, nia) and isonicotinamide (pyridine-4-carboxamide, isn) ligands, together with thiocyanate as the co-ligand in aqueous solutions (water as a possible third ligand). In this work, DFT calculations in the multicomponent system (Ni/SCN/isn/H<sub>2</sub>O) predicted complexes with several different ratios of the ligands. Crystal engineering by a crystallization screening method with varying concentrations of isn gave seven different complexes: three ternary heteroleptic complexes, namely  $[\text{Ni}(\text{NCS})_2(\text{isn})_2(\text{H}_2\text{O})_2] \cdot 2\text{H}_2\text{O}$  (1),  $[\text{Ni}(\text{NCS})_2(\text{isn})_2(\text{H}_2\text{O})_2]$  (2),  $[\text{Ni}(\text{NCS})_2(\text{isn})_3(\text{H}_2\text{O})] \cdot 2.5\text{H}_2\text{O}$  (3), a mixed two/three component complex  $[\text{Ni}(\text{NCS})_2(\text{isn})_3(\text{H}_2\text{O})] \cdot 3[\text{Ni}(\text{NCS})_2(\text{isn})_4] \cdot 9\text{H}_2\text{O}$  (4), and three two-component ones  $[\text{Ni}(\text{NCS})_2(\text{isn})_4] \cdot 3\text{H}_2\text{O}$  (5),  $[\text{Ni}(\text{NCS})_2(\text{isn})_4] \cdot 2(\text{isn})$  (6) and  $[\text{Ni}(\text{NCS})_2(\text{isn})_4] \cdot 1.25\text{H}_2\text{O}$  (7). 6 is a co-crystal and has channels in the structure that can accommodate different molecules. We

decided to include 5 in our paper since it was obtained by a different synthetic route than reported previously<sup>23</sup> and we have discussed its structure from a different point of view. The aim of this research was to put more light on the correlation between nickel as a biologically active metal with isonicotinamide, thiocyanate and water as ligands of biological importance with the emphasis on synthesis, crystal structure, intermolecular interactions, and DFT calculations.

## Experimental section

### Materials and preparation of complexes

All chemicals were purchased from Aldrich Chemical Co. and were used as received without further purification. The CHN-microanalyses were performed in a Perkin-Elmer 2400 Series II CHNS analyser in the Chemical Analytical Service Laboratories of the Ruder Bošković Institute, Zagreb, Croatia.

### Crystallization screening

After standard crystallization trials using Ni:SCN:isn molar ratios from 1:2:1 to 1:2:4, crystals of different complexes were obtained (3, 5, and 6), often within the same beaker. It became evident that a “finer” screening was necessary. 96 well plastic plates were used for batch crystallization screening. Stocks of aqueous solutions were made: 1.0 mol dm<sup>-3</sup> nickel(II) nitrate hexahydrate, 2.0 mol dm<sup>-3</sup> potassium thiocyanate and 0.5 mol dm<sup>-3</sup> isonicotinamide. They were added in 32 wells (one plate was used for three separate experiments) in the following order to a total of 100  $\mu\text{L}$ : water, nickel nitrate, potassium thiocyanate, isonicotinamide. The concentrations of nickel (0.05 mol dm<sup>-3</sup>) and thiocyanate (0.10 mol dm<sup>-3</sup>) were kept constant while the concentration of isonicotinamide was lowered by 0.01 mol dm<sup>-3</sup> in each following reservoir, from 0.35 to 0.04 mol dm<sup>-3</sup>. Columns in the plate were labelled 1–8 and rows A to D. Each set of 32 reservoirs was covered with adhesive plastic foil and kept at 22(1) °C. Each plate was checked every few days and pictures were taken after an hour, one day, two weeks and one month (Fig. 1 and S1,† Scheme 1, and Table S1†). The crystals were analysed by PXRD (Fig. S2†). In the last screen, isonicotinamide was added before potassium thiocyanate to check if the order of addition of reactants can influence the

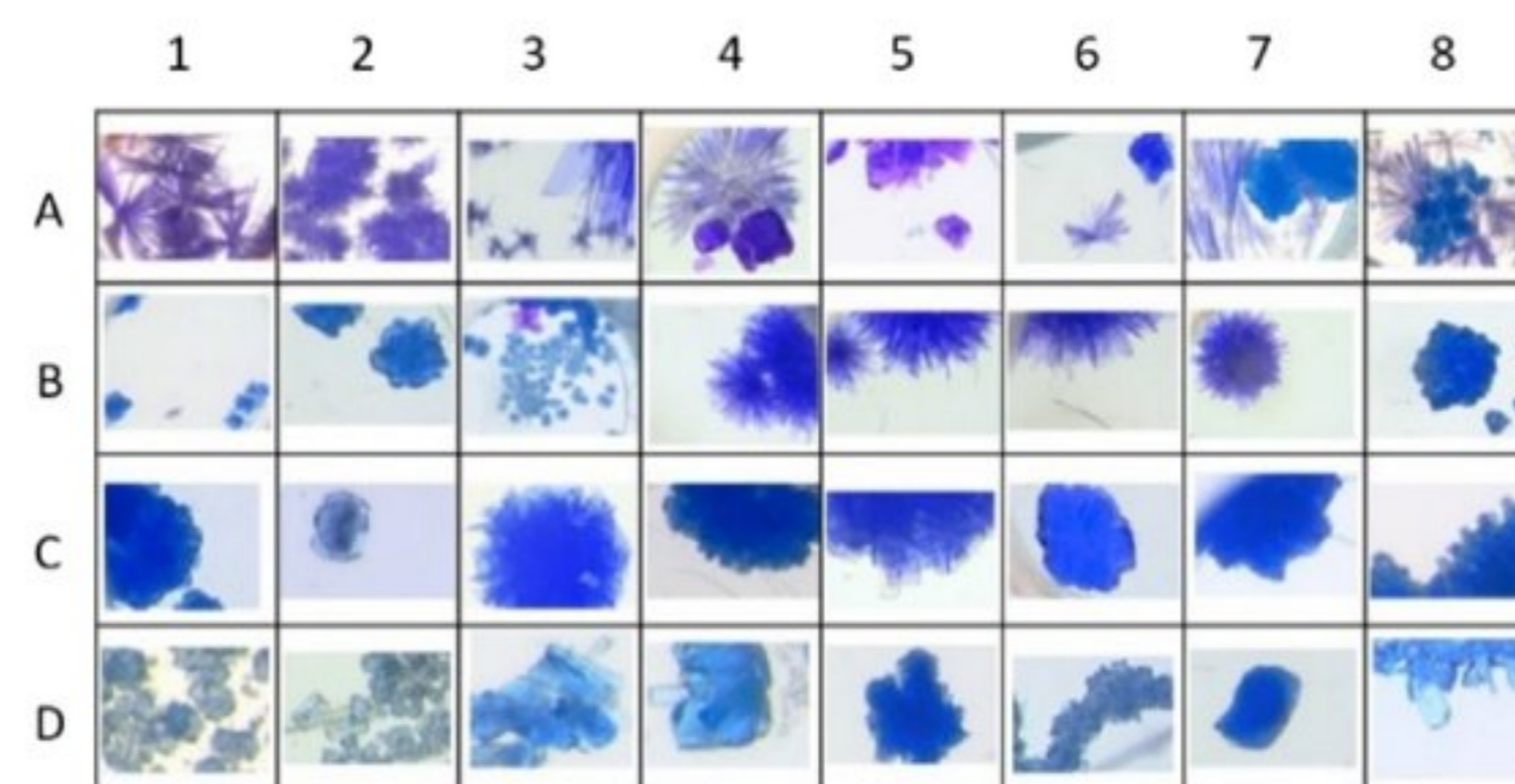
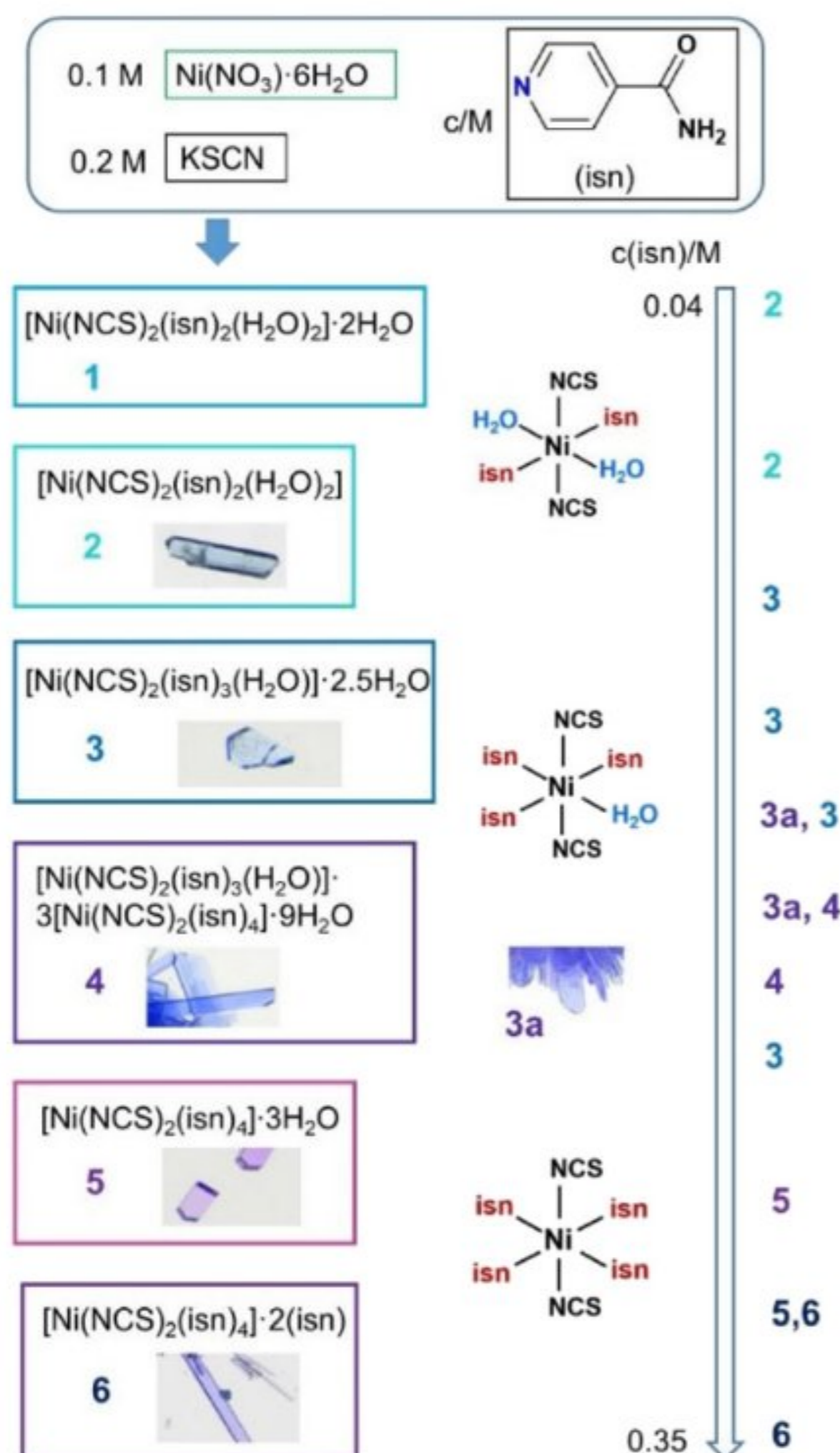


**Fig. 1** Crystallization screening results. The containers are labelled 1–8 horizontally, and A–D vertically (A1 contains 0.35 M and D8 0.04 M isonicotinamide).



**Scheme 1** Crystallization screening results and molar ratios of reactants for the synthesis.

crystallization of the complexes. One plate was made using the Oryx 8 robot.<sup>24</sup>

**[Ni(NCS)<sub>2</sub>(isn)<sub>2</sub>(H<sub>2</sub>O)<sub>2</sub>]<sub>2</sub>·2H<sub>2</sub>O (1).** An aqueous solution of isonicotinamide (0.24 g; 2 mmol; 50 mL) was added dropwise into an aqueous solution of nickel(II) nitrate hexahydrate (0.29 g; 1 mmol; 10 mL). The reaction mixture was thoroughly stirred and into this mixture an aqueous solution of potassium thiocyanate (0.18 g; 2 mmol; 10 mL) was added. The resulting solution was left at room temperature and after a few days blue crystals were formed. Yield: 69% (0.340 g). Anal. calc. for C<sub>14</sub>H<sub>20</sub>N<sub>6</sub>NiO<sub>6</sub>S<sub>2</sub>: C, 34.23; H, 4.10; N, 17.11; S, 13.06%. Found: C, 34.52; H, 4.21; N, 17.30; S, 13.16%. <sup>1</sup>H NMR, δ [ppm] (DMF-*d*<sub>7</sub>), (Δ<sub>v<sub>1/2</sub></sub> [Hz]): 7.93 (60), 8.68 (270), 38.7 (1500), 114 (7986).

**[Ni(NCS)<sub>2</sub>(isn)<sub>2</sub>(H<sub>2</sub>O)<sub>2</sub>] (2).** The best crystals were obtained in reservoir D8 of the crystallization screening experiment. It took at least a month to obtain the crystal so this crystallization condition was scaled up without the addition of water. 1 mL of 1.0 mol dm<sup>-3</sup> nickel(II) nitrate hexahydrate was mixed with 1 mL of 2.0 mol dm<sup>-3</sup> potassium thiocyanate, and then 1.56 mL of 0.5 mol dm<sup>-3</sup> isonicotinamide was added dropwise while stirring. The resulting solution was left at room temperature and after one day cyan crystals were formed. They were filtered off. Yield: 64% (0.293 g). Anal. calc. for C<sub>14</sub>H<sub>16</sub>N<sub>6</sub>NiO<sub>4</sub>S<sub>2</sub>: C, 36.94; H, 3.54; N, 18.46; S, 14.09%. Found: C, 36.72; H, 3.71; N, 18.50; S, 14.16%. <sup>1</sup>H NMR, δ [ppm] (DMF-*d*<sub>7</sub>), (Δ<sub>v<sub>1/2</sub></sub> [Hz]): 7.91 (n.d.), 8.58 (241), 38.9 (1596), 120.1 (6800).

**[Ni(NCS)<sub>2</sub>(isn)<sub>3</sub>(H<sub>2</sub>O)]·2.5H<sub>2</sub>O (3).** An aqueous solution of isonicotinamide (0.24 g; 2 mmol; 50 mL) was added dropwise

into an aqueous solution of nickel(II) nitrate hexahydrate (0.29 g; 1 mmol; 10 mL). The reaction mixture was thoroughly stirred and into this mixture an aqueous solution of potassium thiocyanate (0.18 g; 2 mmol; 10 mL) was added. The resulting solution was left at room temperature and left to evaporate. After a few days purple plate-like crystals (labelled 3a) were obtained along with a few violet crystals of 6 which were of good quality for X-ray analysis. When a few crystals of 3a were taken out of the solution, they cracked and decomposed immediately. If left in the solution, they dissolved and light blue stable crystals of 3 were obtained. They were filtered off. Crystals of 3 were also obtained from the scaled up condition C2 of the crystallization screening experiment. 100 μL of 1.0 mol dm<sup>-3</sup> nickel(II) nitrate hexahydrate was mixed with 100 μL of 2.0 mol dm<sup>-3</sup> potassium thiocyanate and 1.08 mL of water, and then 720 μL of 0.5 mol dm<sup>-3</sup> isonicotinamide was added dropwise while stirring. The resulting solution was left at room temperature and after one day light blue crystals were formed. They were filtered off. Yield: 86% (0.104 g). Anal. calc. for C<sub>20</sub>H<sub>25</sub>N<sub>8</sub>NiO<sub>6.5</sub>S<sub>2</sub>: C, 39.75; H, 4.17; N, 18.54; S, 10.61%. Found: C, 39.78; H, 4.31; N, 18.61; S, 10.71%. <sup>1</sup>H NMR, δ [ppm] (DMF-*d*<sub>7</sub>), (Δ<sub>v<sub>1/2</sub></sub> [Hz]): 8.01 (88.5), 8.69 (103), 39.25 (1920), 114.3 (7996).

**[Ni(NCS)<sub>2</sub>(isn)<sub>3</sub>(H<sub>2</sub>O)]·3[Ni(NCS)<sub>2</sub>(isn)<sub>4</sub>]·9H<sub>2</sub>O (4).** Blue crystals of 4 were formed from 3a in B3, B5 and B6 reservoirs of the crystallization screening experiments after the foil was removed for a short time to take a crystal for X-ray diffraction analysis (B6: 5 μL of 1.0 mol dm<sup>-3</sup> nickel(II) nitrate hexahydrate was mixed with 5 μL of 2.0 mol dm<sup>-3</sup> potassium thiocyanate and 45 μL water) and then 44 μL of 0.5 mol dm<sup>-3</sup> isonicotinamide were added. They were taken out and dried on a filter paper. Yield: 83% (0.005 g). Anal. calc. for C<sub>98</sub>H<sub>110</sub>N<sub>38</sub>Ni<sub>4</sub>O<sub>25</sub>S<sub>8</sub>: C, 43.41; H, 4.09; N, 19.63; S, 9.46%. Found: C, 43.52; H, 4.15; N, 19.71; S, 9.61%.

**[Ni(NCS)<sub>2</sub>(isn)<sub>4</sub>]·3H<sub>2</sub>O (5).** Purple crystals of 5 were isolated from the light blue solution remaining after filtering off the crystals of 6 (see below). 5 was also obtained as the only product in the A5 reservoir of one crystallization screening experiment. The stable crystals were taken out and dried on a filter paper. Yield: 90% (0.0035 g). Anal. calc. for C<sub>26</sub>H<sub>30</sub>N<sub>10</sub>NiO<sub>7</sub>S<sub>2</sub>: C, 43.53; H, 4.22; N, 19.52; S, 8.94%. Found: C, 43.61; H, 4.30; N, 19.65; S, 8.97%. <sup>1</sup>H NMR, δ [ppm] (DMF-*d*<sub>7</sub>), (Δ<sub>v<sub>1/2</sub></sub> [Hz]): 7.84 (120), 8.50 (166), 39.1 (1584), 116.5 (8986).

**[Ni(NCS)<sub>2</sub>(isn)<sub>4</sub>]·2(isn) (6).** An aqueous solution of nickel(II) nitrate hexahydrate (0.29 g; 1 mmol; 10 mL) was mixed with an aqueous solution of potassium thiocyanate (0.18 g; 2 mmol; 5 mL) and an aqueous solution of isonicotinamide (0.60 g; 5.0 mmol; 35 mL) was added while stirring at room temperature. Violet crystals precipitated and were filtered off. Since these crystals precipitated quickly, they were not suitable for X-ray diffraction analysis. Yield: 92% (0.831 g). Anal. calc. for C<sub>38</sub>H<sub>36</sub>N<sub>14</sub>NiO<sub>6</sub>S<sub>2</sub>: C, 50.29; H, 4.00; N, 21.61; S, 7.07%. Found: C, 50.34; H, 4.08; N, 21.72; S, 6.99%. Complex 6 was also always obtained as the only product in reservoir

A1 of the crystallization screening experiment.  $^1\text{H}$  NMR,  $\delta$  [ppm] (DMF- $d_7$ ), ( $\Delta\nu_{1/2}$  [Hz]): 7.80 (112), 8.45 (118), 8.75 (n.d.), 39.0 (1584), 116.4 (8908).

**[Ni(NCS) $_2$ (isn) $_4$ ]-1.25H $_2$ O (7).** Blue crystals were obtained in reservoir B2 of the crystallization screening experiment where potassium thiocyanate was added after isonicotinamide. They were taken out of the reservoir and dried on a filter paper. There were enough crystals only for PXRD and the single-crystal X-ray experiment.

### Single-crystal X-ray structure determination

A suitable single crystal of **1** was selected and glued to a thin glass fibre. Data collection was performed at room temperature on an Oxford Diffraction Xcalibur four-circle kappa geometry diffractometer with the Xcalibur Sapphire 3 CCD detector, using graphite-monochromated MoK $\alpha$  ( $\lambda = 0.71073$  Å) radiation with the CrysAlisPro Software ver. 1.171.37.33<sup>25a</sup> for data reduction. Crystals of **2–7** were mounted on cryo-loops with some Paratone N oil and the data were collected at 170 K on a Rigaku XtaLAB Synergy (Dualflex, HyPix) diffractometer using CuK $\alpha$  ( $\lambda = 1.54184$  Å) radiation. Data were reduced by the CrysAlisPro 1.171.41.92a (Rigaku Oxford Diffraction, 2020) program.<sup>25b</sup> All X-ray diffraction data were corrected for the Lorentz-polarization factor and absorption effects by the multi-scan method. All structures were solved by direct methods with SHELXS or SHELXT<sup>26</sup> within the OLEX program.<sup>27</sup> Coordinates and anisotropic displacement parameters for all non-hydrogen atoms were refined by full-matrix least-squares methods based on  $F^2$  values by SHELXL.<sup>28</sup> The C–H and N–H hydrogen atoms were positioned in calculated positions with  $U_{\text{iso}}(\text{H}) = 1.2U_{\text{eq}}(\text{C}, \text{N})$  using a riding model with C–H = 0.95 Å for aromatic and N–H = 0.88 Å for amide H atoms. Water hydrogens were located in the difference-Fourier map and refined using DFIX distance restraints with O–H = 0.85 Å, H1–H2 = 1.37 Å and  $U_{\text{iso}}(\text{H}) = 1.5U_{\text{eq}}(\text{O})$ . The disordered water molecule O3 in **3** has the oxygen atom split in two positions close to each other (O3A–O3B = 0.82(3) Å). Their occupancies were refined to 0.685(12) and 0.315(12) for O3A and O3B, respectively. Molecular geometry and intermolecular interaction calculations were performed using PLATON.<sup>29,30</sup> The molecular graphics were done using ORTEP-3,<sup>31</sup> MERCURY-3.8<sup>32</sup> and VESTA-3.2.1.<sup>33</sup> Relevant information on the crystal data, data collection, and refinement are compiled in Table S2.†

### Powder X-ray diffraction

Powder X-ray diffraction (PXRD) was performed on a Malvern Panalytical Aeris diffractometer in the Bragg–Brentano geometry with CuK $\alpha$  radiation ( $\lambda = 1.54184$  Å) at room temperature. The samples were placed on a silicon holder and the diffractograms were measured in the  $2\theta$  range 5–40° with a step size of 0.022° and 15.0 s per step. Powder X-ray diffraction data were collected and visualized using the HighScore Plus program.<sup>34</sup>

### NMR spectroscopy

All  $^1\text{H}$  NMR spectra were recorded on Bruker AV500 (**1**) and Bruker AV600 spectrometers (**2–6**) equipped with 5 mm diameter probes with z-gradient accessory. All samples were dissolved in DMF- $d_7$ . The residual high-field solvent signal at 2.75 ppm for  $^1\text{H}$  was used as a reference. The spectra of the paramagnetic Ni(II) complexes were acquired using the following parameter values: sweep width of 200 ppm, transmitter frequency offset of 70.0 ppm, a relaxation delay of 1 s, an acquisition time of 0.82 s, matrix sizes of 80 K (acquisition) and 64 K (FT), and 64 scans. The half-widths of the signals ( $\Delta\nu_{1/2}$ , Hz) were read at half the signal height. Despite the long acquisition, no  $^{13}\text{C}$  NMR signals were detected, except those from the solvent. The n.d. (not detected) mark in the NMR assignments indicates that the overlap of signals prevents measurement of this value.

### Thermal measurements

Thermal measurements for **1** were performed on a Mettler-Toledo TGA/SDTA 851e analyser at a heating rate of 10 °C min $^{-1}$  in a nitrogen atmosphere at a flow rate of 50 mL min $^{-1}$  in the temperature range 25–600 °C, and for **2–6** on a Mettler-Toledo TGA/DSC3+ instrument at a heating rate of 10 °C min $^{-1}$  in an oxygen atmosphere and a flow rate of 50 mL min $^{-1}$  in the temperature range 25–800 °C (**4** and **6**) or 25–1000 °C (**2**, **3** and **5**). 1–10 mg of samples was placed in alumina crucibles (70  $\mu\text{L}$ ).

### IR spectroscopy

Infrared spectra were recorded as KBr pellets in the range 4000–450 cm $^{-1}$  on a Perkin-Elmer Spectrum RXI FT-spectrometer.

### Computational details

All molecular geometries were optimized by the modern long-range corrected hybrid  $\omega\text{B97X-D}$  DFT functional with included empirical dispersion corrections,<sup>35</sup> consistently employing the LANL2DZ basis set for all atoms. Thermal Gibbs free energy corrections were extracted from the frequency calculations and used without the scaling factors. Also, during geometry optimization we included the implicit SMD solvation with all parameters for pure water, in line with our earlier reports that used the same approach to interpret solid-state features of a variety of metal complexes.<sup>36–38</sup> As such, all reported values correspond to solution-phase Gibbs free energies at room temperature (298.15 K) and normal pressure (1 atm) and include both the electronic and the solvation components. Accordingly, the presented interaction energies ( $\Delta G_{\text{INT}}$ ) are calculated as a difference between the total Gibbs free energy of the complex and those from its components. Atomic charges were obtained through the natural bond orbital (NBO) analysis<sup>39</sup> by the same model. All calculations were performed using the Gaussian 16 software.<sup>40</sup> To evaluate intermolecular

interactions within complexes, we performed Hirshfeld surface analysis through the CrystalExplorer 21.5 software,<sup>41</sup> which allowed us to generate a set of 2D fingerprint plots and calculate the enrichment ratios of the matching contacts, in line with literature recommendations.<sup>42,43</sup>

## Results and discussion

### Synthesis of complexes

Complexes 1–7 were prepared at room temperature in an aqueous solution of nickel(II) nitrate hexahydrate and potassium thiocyanate in the molar ratio 1:2, with isonicotinamide in different molar ratios. In all repeated attempts to obtain 1 by this approach, 3 was obtained (the described syntheses are the same), suggesting that 1 might be a metastable product or the exact conditions for its generation were not met. Yet, in the same reaction solution, different products were noticed during evaporation: violet-blue crystals of 3a formed at the bottom, while violet crystals of 6 floated on the surface. If left to evaporate, 3a and 6 disappeared, and blue crystals of 3 formed. In another experiment, we missed 3a, but 5 appeared before 3. The appearance of different products during evaporation was difficult to control, which is why the crystallization screening plate was sealed with a plastic transparent tape to prevent evaporation. The results of one crystallization trial are shown in Fig. 1 and S1.† The concentrations used for setting up the screen and the final screen concentrations are given in Tables S1.1 and S1.2,† respectively. The results of several screenings are summarised in Scheme 1.

In that way, two new complexes were found, 2 and 4. Cyan crystals of 2 appeared in the wells with very low concentrations of isonicotinamide, while 3a crystallized in wells B3, B5 and B6. The reservoirs were opened for a few minutes and a crystal of 3a was taken from each well, but they instantly decomposed when exposed to air. Interestingly, the 3a crystals remaining in the solution later transformed to 4. 3a was also obtained once in C5. When repeated twice, this experiment did not end with the same compounds in the same wells. 2 always appeared in D6–D8 and 6 in A1–A2. Complex 5 was obtained at higher isonicotinamide concentrations, mostly together with 6 (A4–A8). Combinations of 3 and 6 were in A6–B1, and 3 and 5 in A6–B3. Complex 3 was found in the majority of reservoirs (B1–C8). Seeding was also attempted in order to get more crystals of 4. Compounds 2 and 5 were tested to see if they can also crystallize with other isonicotinamide concentrations. Conditions B5 and C5 were scaled up 50× in a glass beaker and divided into three equal volumes. Seeds of 2, 4 and 5 were added, one in each, and sealed with parafilm. In the beakers where 2 or 4 were added, only 3 crystallized, while in those where 5 was added, both 3 and 5 crystallized. Thus, the nucleation within these conditions depends on the container type (plastic, glass), size, and volume since mixing is different in small and big volumes. It was noticed that nucleation can appear locally where isonicotinamide is added even while

mixing. 7 crystallized in the last crystallization screen where potassium thiocyanate was added after isonicotinamide, but the appearance of 2, 3, 5 and 6 was as usual. In contrast to our synthesis in the aqueous solution, Wicht *et al.* obtained  $[\text{Ni}(\text{NCS})_2(\text{isn})_4]$  by adding isonicotinamide to nickel isothiocyanate in a 1:1 molar ratio in ethanol and by stirring overnight.<sup>23</sup> To obtain 5, the host,  $[\text{Ni}(\text{NCS})_2(\text{isn})_4]$ , was dissolved in water. 6 could not be obtained by this procedure since an ethanolic solvate, 6·EtOH, crystallized.

### Crystal structures

In all structures, nickel(II) ions are octahedrally coordinated by two *trans* N-coordinating thiocyanates resulting in neutral complexes, with a different number of isn ligands, and in 1–4 also by coordinated water oxygen atoms. In the packing arrangements, the adjacent molecules are interconnected by hydrogen bonding and other non-covalent interactions. Selected dihedral angles between pyridine rings and amide groups are given in Table S3,† and the interatomic distances (Å) and angles (°) of the complexes are listed in Tables S4 and S5.† Additional analysis and discussion of the molecular structures is given in paragraph S1.† Observed and calculated PXRD patterns are shown in Fig. S2.†

$[\text{Ni}(\text{NCS})_2(\text{isn})_2(\text{H}_2\text{O})_2] \cdot 2\text{H}_2\text{O}$  (1). The structure of 1 is monoclinic (space group  $P2_1/c$ ) with the central metal ions lying on the crystallographic centre of inversion. The  $\text{NiN}_4\text{O}_2$  octahedral coordination of the metal centre is formed by three pairs of symmetry-related atoms (Fig. 2) that are all *trans* to each other: equatorially two water molecule oxygen

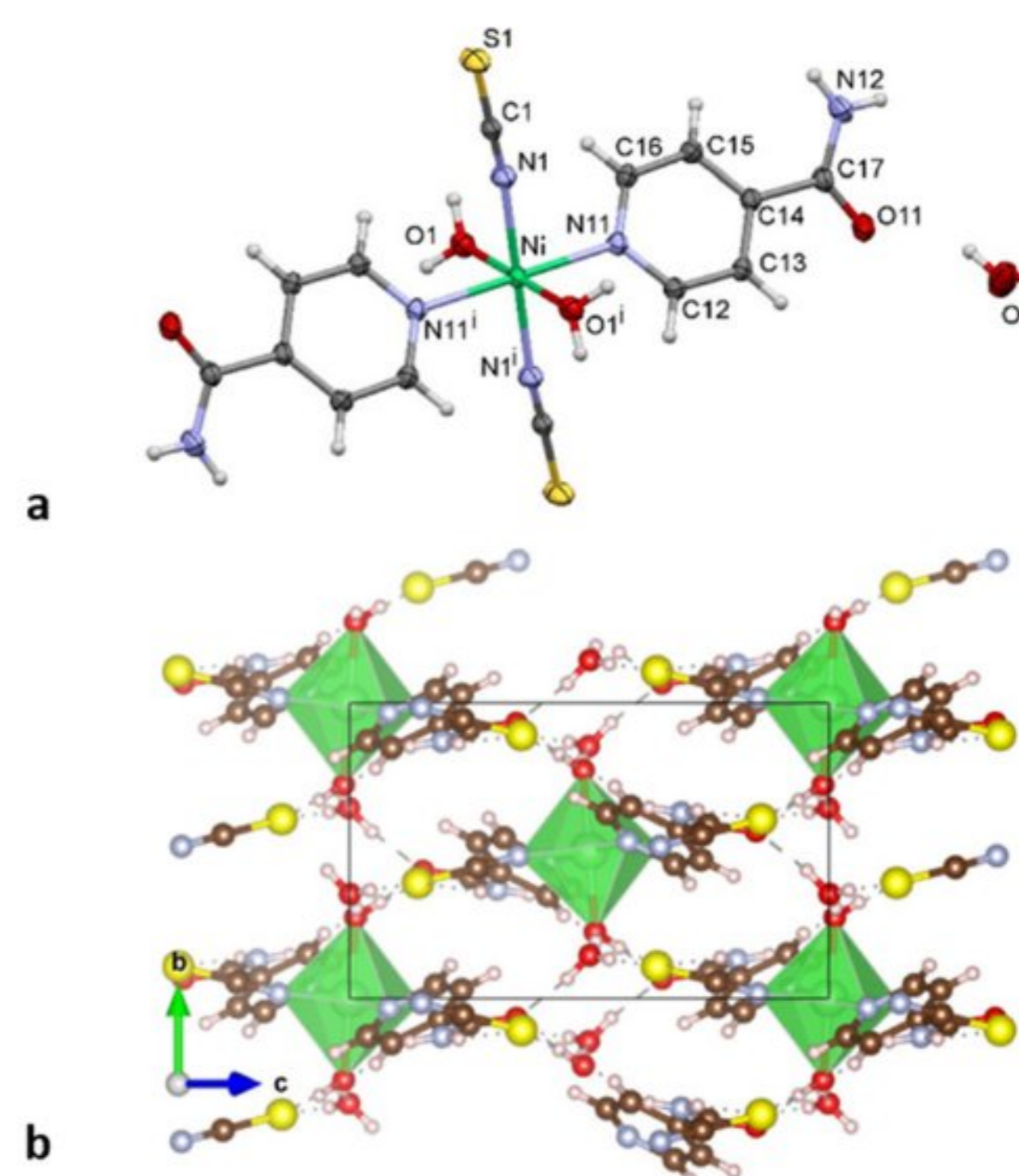


**Fig. 2** Molecular structure of  $[\text{Ni}(\text{NCS})_2(\text{isn})_2(\text{H}_2\text{O})_2] \cdot 2\text{H}_2\text{O}$  (1) with the atom-numbering scheme (symmetry code: (i)  $-x + 1, -y + 1, -z + 1$ ). The thermal ellipsoids are drawn at the 50% probability level (a). Crystal packing of 1 viewed down the *a*-axis showing the hydrogen bond pattern represented by dashed ( $\text{O} \cdots \text{H}$  interactions) and dotted ( $\text{S} \cdots \text{H}$  interactions) lines (b).

**Table 1** Selected bond distances (Å) in the coordination octahedra of Ni(II) complexes 1–6

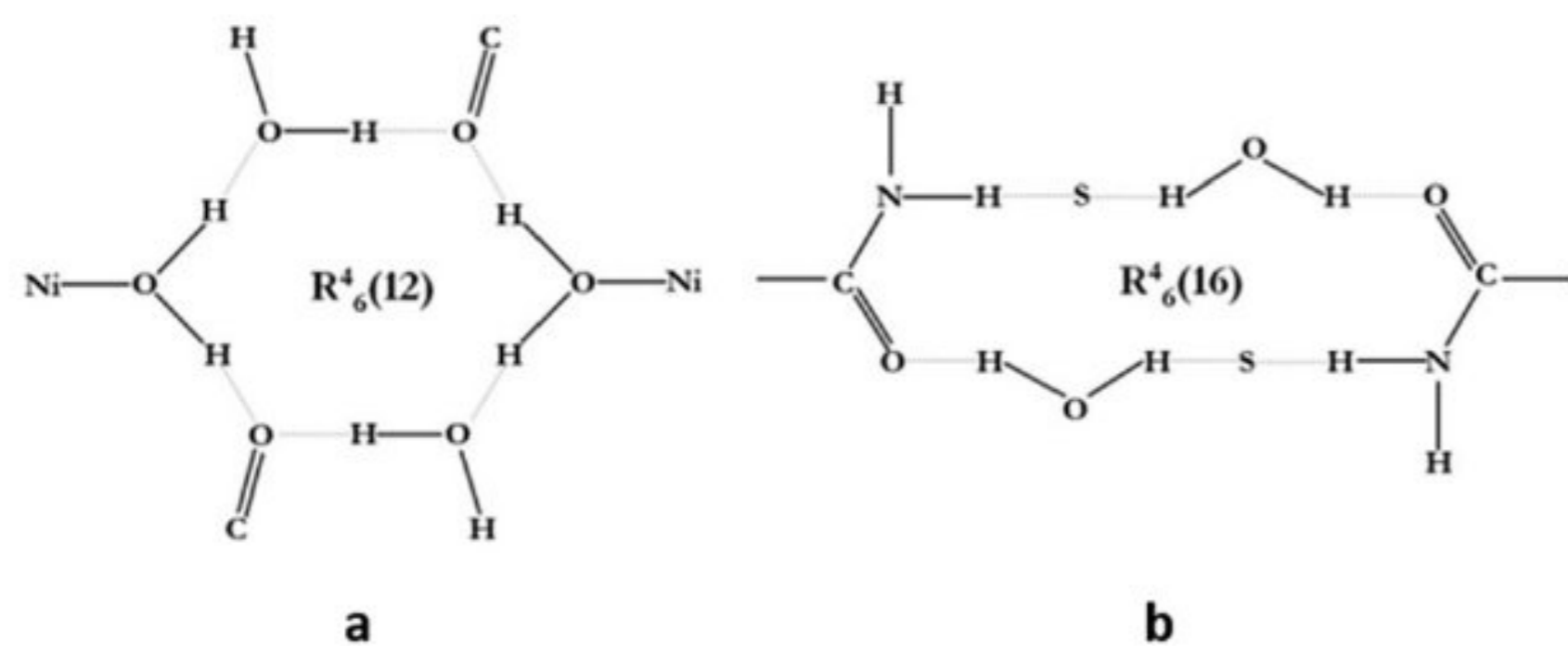
	1	2	3	4(Ni1)	4(Ni2)	4(Ni3)	4(Ni4)	5	6
Ni–O <sub>w</sub>	2.0838(14) × 2	2.1055(10) × 2	2.137(2)	2.126(3)	—	—	—	—	—
Ni–N <sub>isn</sub>	2.1268(17) × 2	2.1126(10) × 2	2.166(3)	2.103(4)	2.108(3)	2.110(3)	2.114(3)	2.1238(11) × 2	2.1305(11)
			2.115(2)	2.131(4)	2.112(3)	2.137(3)	2.116(3)	2.1131(11) × 2	2.1231(12)
			2.119(2)	2.133(4)	2.126(3)	2.138(3)	2.129(3)		2.1276(11)
					2.126(3)	2.145(3)	2.142(3)		2.1247(12)
Ni–N <sub>NCS</sub>	2.0461(16) × 2	2.0421(12) × 2	2.045(3)	2.037(4)	2.056(4)	2.044(4)	2.051(3)	2.0555(12) × 2	2.0517(12)
			2.033(2)	2.061(4)	2.076(4)	2.068(4)	2.075(3)		2.0536(12)

O1 atoms with two isothiocyanate nitrogen N1 atoms, and in the axial positions two pyridine ring nitrogen N11 atoms (Table 1).

Each uncoordinated water H<sub>2</sub>O<sub>2</sub> forms three hydrogen bonds: one with the O1 donor oxygen of the coordinated water (O1⋯O2<sup>iii</sup> = 2.7920(2) Å, symmetry code: (iii)  $x, 1/2 - y, -1/2 + z$ ), another with the isonicotinamide O11 oxygen (O2⋯O11 = 2.7621(3) Å), and finally with thiocyanate S1 sulphur (O2⋯S1<sup>viii</sup> = 3.339(3) Å, symmetry code: (viii)  $-x + 1, -y + 1, -z + 2$ ) forming O–H⋯S interactions. The same thiocyanate S1 sulphur accepts an additional amide hydrogen atom (N12⋯S1<sup>vi</sup> = 3.4731(2) Å, symmetry code: (vi)  $x - 1, y, z$ ) and a pyridine hydrogen atom (C15⋯S1<sup>vii</sup> = 3.641(2) Å, symmetry code: (vii)  $x - 1, -y + 3/2, z - 1/2$ ) from neighbouring molecules. The coordinated H<sub>2</sub>O<sub>1</sub> water also participates in additional O1–H⋯O11<sup>v</sup> hydrogen bonding with the amide group (O1⋯O11<sup>v</sup> = 2.7806(2) Å, symmetry code: (v)  $1 - x, -1/2 + y, 3/2 - z$ ).

Both the coordinated and the uncoordinated waters participate in the hydrogen bonding in similar ways (Fig. 2b). The O–H⋯O, N–H⋯O, N–H⋯S and C–H⋯S hydrogen bonding interactions are established. No typical amide–amide dimers R<sub>2</sub><sup>2</sup>(8) (Scheme S1a†) or thiocyanate tetramers R<sub>4</sub><sup>2</sup>(8), but interesting new hexamer motifs of R<sub>6</sub><sup>4</sup>(12) and R<sub>6</sub><sup>4</sup>(16), were observed.

Hexamers R<sub>6</sub><sup>4</sup>(12) (Scheme 2a) consist of two coordinated and two co-crystallized waters and two amide oxygens. These hexamers are doubly fused by two centrosymmetric R<sub>6</sub><sup>4</sup>(16) rings (Scheme 2b), thus providing additional stabilization to the co-crystallized waters and forming an infinite 3D hydrogen bonding framework. The analysis of short ring–ring distances which are typical for stacking (approximately 3.0–



**Scheme 2** Hexamer R<sub>6</sub><sup>4</sup>(12) (a) and centrosymmetric R<sub>6</sub><sup>4</sup>(16) (b) ring involving two coordinated H<sub>2</sub>O<sub>1</sub> waters, two amide O11 oxygens and two co-crystallized H<sub>2</sub>O<sub>2</sub> waters observed in 1.

4.0 Å) showed that the C<sub>g</sub>1⋯C<sub>g</sub>1<sup>ix</sup> distance of 5.2108(3) Å is quite long (symmetry code: (ix)  $1 - x, -1/2 + y, 1/2 - z$ ).

[Ni(NCS)<sub>2</sub>(isn)<sub>2</sub>(H<sub>2</sub>O)<sub>2</sub>] (2). The molecular structure of 2 is similar to that of 1, which is the hydrate form, with only somewhat different geometrical parameters (Tables 1 and S3–S5†). Typical head-to-head amide–amide hydrogen bond R<sub>2</sub><sup>2</sup>(8) dimers, linked to two combined R<sub>4</sub><sup>2</sup>(8) tetramers sharing N–H⋯O hydrogen bonds, were found in 2 (Fig. 3 and Scheme 3). Each combined R<sub>4</sub><sup>2</sup>(8) tetramer involves a coordinated water H<sub>2</sub>O<sub>1</sub> oxygen and amide N12 as double donors, where the carboxamide O11 oxygen and the terminal thiocyanate S1 sulphur act as bifurcated hydrogen bond acceptors for two hydrogen bonding interactions. Additionally, the terminal thiocyanate sulphur acts as an acceptor for one weak C–H⋯S hydrogen bonding. The pyridine rings are interlinked by the π-stacking C<sub>g</sub>1⋯C<sub>g</sub>1<sup>vii</sup> contacts of 3.7626(1) Å, (symmetry code: (vii)  $x, 1/2 - y, 1/2 + z$ ).

[Ni(NCS)<sub>2</sub>(isn)<sub>3</sub>(H<sub>2</sub>O)]·2.5H<sub>2</sub>O (3). Complex 3 is isostructural with [Co(NCS)<sub>2</sub>(isn)<sub>3</sub>(H<sub>2</sub>O)]·2.5H<sub>2</sub>O,<sup>19,22</sup> and its asymmetric unit (monoclinic, space group *C2/c*) contains one Ni(II) cation octahedrally coordinated by three isonicotinamides, two thiocyanate anions and a water molecule (Fig. 4), with two co-

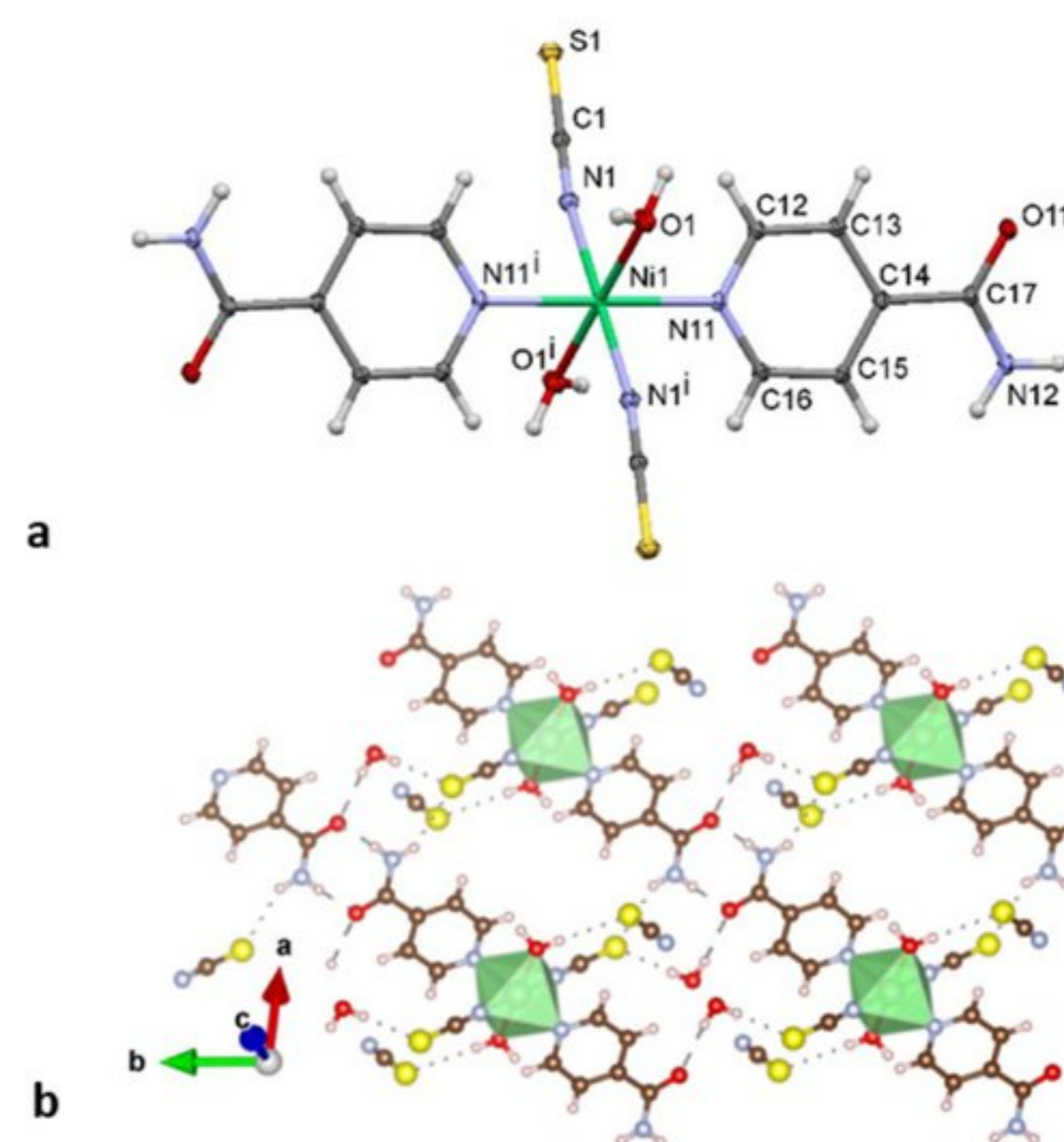
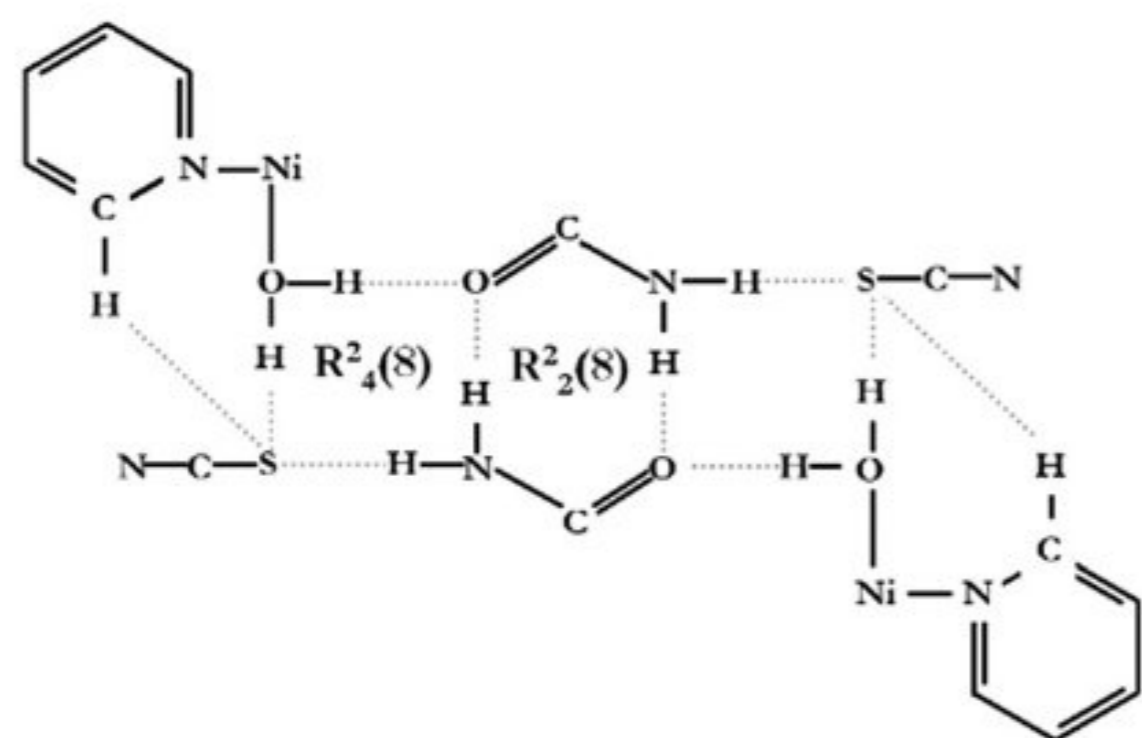


**Fig. 3** Molecular structure of [Ni(NCS)<sub>2</sub>(isn)<sub>2</sub>(H<sub>2</sub>O)<sub>2</sub>] (2) with the atom-numbering scheme (symmetry code: (i)  $-x + 2, -y + 1, -z + 1$ ). The thermal ellipsoids are drawn at the 50% probability level (a). Crystal structure of 2 showing the hydrogen bond pattern represented by dashed (O⋯H interactions) and dotted (S⋯H interactions) lines (b).



**Scheme 3** Hydrogen bonded  $R_2^2(8)$  dimer and combined  $R_4^2(8)$  tetramers of  $[\text{Ni}(\text{NCS})_2(\text{isn})_2(\text{H}_2\text{O})_2]$  (**2**).

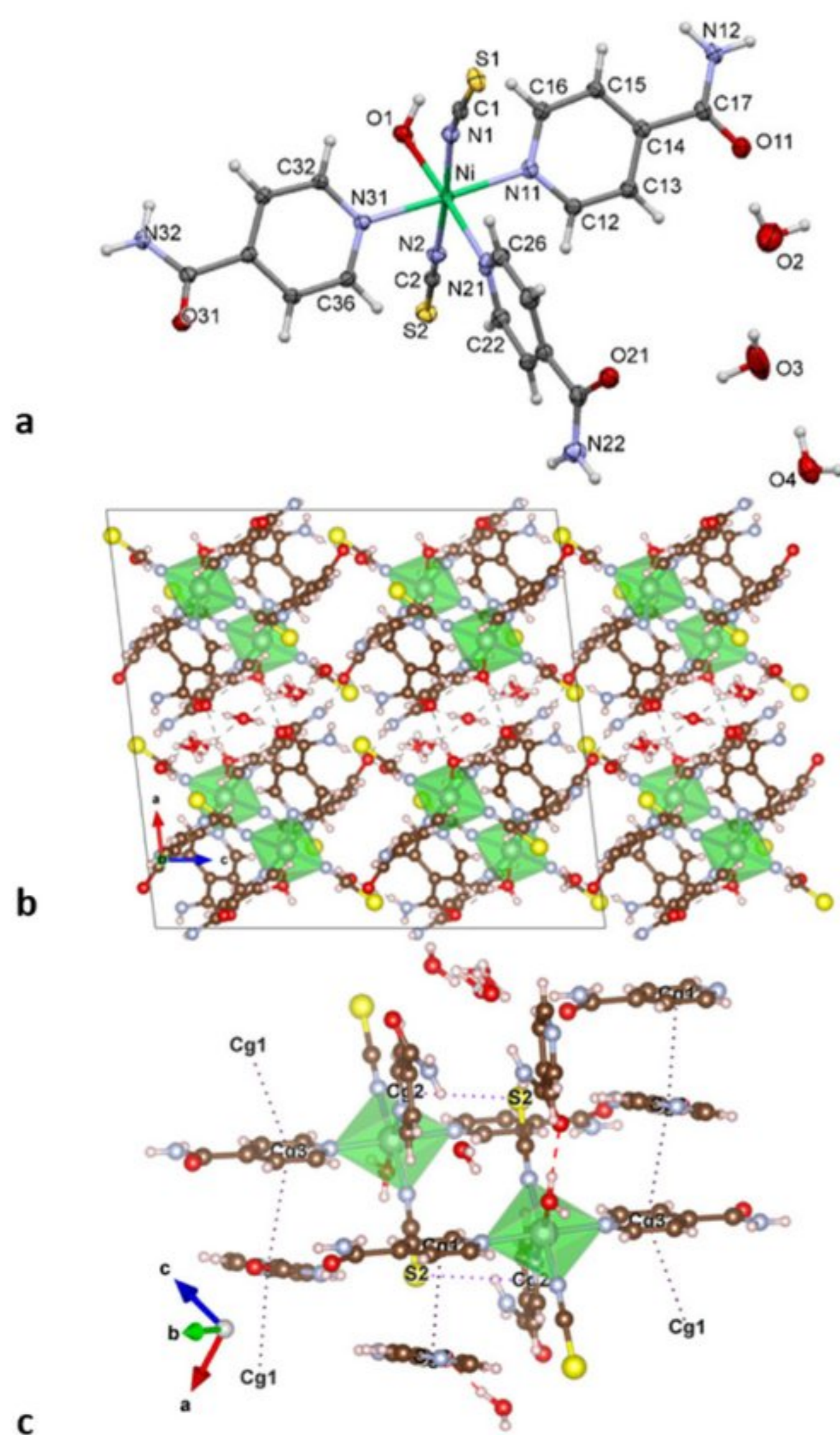


**Fig. 4** Molecular structure of  $[\text{Ni}(\text{NCS})_2(\text{isn})_3(\text{H}_2\text{O})]\cdot 2.5\text{H}_2\text{O}$  (**3**) with the atom-numbering scheme and only one of the disordered waters,  $\text{H}_2\text{O}^3$  (a). Double sheets in the  $(2\ 0\ \bar{2})$  planes (view along the  $b$ -axis) formed by *trans*-related isonicotinamides. Intermolecular hydrogen bonds are shown as dashed lines (b). The  $\pi$ -stacking and sulphur- $\pi$  interactions are marked by dotted lines ( $C_{g1}$ ,  $C_{g2}$  and  $C_{g3}$  are the centroids of the  $\text{N}11\text{C}12\text{--C}16$ ,  $\text{N}21\text{C}22\text{--C}26$  and  $\text{N}31\text{C}32\text{--C}36$  pyridine rings, respectively) (c).

crystallized waters in general positions and one  $\text{H}_2\text{O}$  ( $\text{O}2$ ) located on a twofold rotation axis (special position  $4e$ , site symmetry 2). As in its cobalt analogue, the  $\text{NiN}_5(\text{OH}_2)$  octahedral coordination is formed by three pyridine ring nitrogens  $\text{N}11$ ,  $\text{N}21$ ,  $\text{N}31$  from three isonicotinamides, two thiocyanate nitrogen  $\text{N}1$  and  $\text{N}2$  atoms at slightly shorter distances from two equatorially *trans* N-bonded thiocyanate ligands and one water oxygen  $\text{O}1$  (Table 1).

Both H atoms of the coordinated  $\text{H}_2\text{O}1$  water form two hydrogen  $\text{O}\text{--}\text{H}\cdots\text{O}$  bonds with two symmetry equivalents of

$\text{O}21$  atoms from adjacent isonicotinamides positioned *trans* to it. Thus, the amide  $\text{O}21$  oxygen acts as a bifurcated hydrogen bond acceptor. Two such hydrogen bonding interactions form an  $R_4^2(8)$  ring (Scheme  $\text{S}1\text{c}^\dagger$ ). Additionally, the same amide  $\text{O}21$  oxygen accepts a hydrogen atom from one more, much weaker  $\text{C}\text{--}\text{H}\cdots\text{O}$  hydrogen bonding interaction. Consequently, slight elongation of the amide  $\text{C}\text{--}\text{O}$  bond was observed due to the trifurcated acceptor action of the  $\text{O}21$  oxygen.

The complex molecules are packed in such a way that *trans*-related isonicotinamides form double sheets in the  $(2\ 0\ \bar{2})$  planes with the thiocyanates directed almost perpendicularly (Fig. 4b). These double sheets are bonded by hydrogen bonds and other noncovalent interactions, forming a complex network. Typical head-to-head  $R_2^2(8)$  amide–amide hydrogen bond dimers (Scheme  $\text{S}1\text{a}^\dagger$ ) are not found. Instead, the already mentioned hydrogen bond ring pattern is formed by the coordinated  $\text{H}_2\text{O}1$  water as a donor and the carboxamide  $\text{O}21$  oxygen atoms as acceptors (Scheme  $\text{S}1\text{c}^\dagger$ ).

The  $\text{O}2$  oxygen of the co-crystallized water  $\text{H}_2\text{O}2$  is the only atom in this structure situated at the special position. It forms two equally long hydrogen bonds  $\text{O}2\text{--}\text{H}\cdots\text{O}11$  with two symmetry equivalents of the amide  $\text{O}11$  atom from adjacent isonicotinamides. The disordered water  $\text{H}_2\text{O}3$ , containing the  $\text{O}$  atom split in two positions close to each other ( $\text{O}3\text{A}\text{--}\text{O}3\text{B} = 0.82(3)$  Å with 68.5(1)% and 31.5(1)% for  $\text{O}3\text{A}$  and  $\text{O}3\text{B}$ ), serves as a hydrogen bond donor to the water  $\text{O}2$  and  $\text{O}4$  and to the amide  $\text{O}11$  and  $\text{O}31$  atoms of the adjacent isonicotinamides. Because of the positional disorder of  $\text{O}3\text{A}$  and  $\text{O}3\text{B}$ , H atoms bound to them are also positionally disordered and it was not possible to precisely locate their positions. Therefore, these H atoms were not included in the refinement. The water H atoms of the co-crystallized water  $\text{H}_2\text{O}4$  form classical  $\text{O}\text{--}\text{H}\cdots\text{O}$  hydrogen bonds with the nearby disordered water  $\text{H}_2\text{O}3$ . The same water  $\text{H}_2\text{O}4$  also creates weak  $\text{O}\text{--}\text{H}\cdots\text{N}$  hydrogen bonding interactions with the thiocyanate and pyridine ring nitrogens ( $\text{N}2$  and  $\text{N}31$ ) as acceptors. In addition, amide H atoms assemble  $\text{N}\text{--}\text{H}\cdots\text{O}$  hydrogen bonds with water oxygen  $\text{O}4$  as well as with amide  $\text{O}31$  acceptor atoms. The amide H atoms additionally form  $\text{N}\text{--}\text{H}\cdots\text{S}$  interactions with  $\text{S}1$  and  $\text{S}2$  atoms of the anionic thiocyanates, which are also involved in forming ring patterns generated with the hydrogen bonds. Two rings (Scheme  $\text{S}1\text{d}^\dagger$ ), which have one common amide group  $\text{--}\text{C}(=\text{O}21)\text{N}22\text{H}_2$ , can be described by the graph-set descriptors  $R_2^2(10)$  and  $R_4^2(14)$ . The anionic thiocyanate ligand  $\text{NCS}1$  belongs to the  $R_4^3(14)$  ring, while the other thiocyanate ligand  $\text{NCS}2$  belongs to the  $R_2^2(10)$  ring. With the nearly planar and parallel to the  $(010)$  plane tetramer  $R_4^2(8)$  in the centre,  $R_4^3(14)$  and  $R_2^2(10)$  are incorporated into the complex pattern (Scheme  $\text{S}1\text{d}^\dagger$ ) where both  $\text{S}1$  and  $\text{S}2$  atoms act as single acceptors. The  $\text{S}2$  atoms are additionally involved as double acceptors in another complex ring of the hydrogen bonding (graph-set descriptor  $R_{10}^6(24)$ ), which is constructed by all three amide groups (Scheme  $\text{S}1\text{e}^\dagger$ ). Two of them,  $\text{--}\text{C}(=\text{O}11)\text{N}12\text{H}_2$  and  $\text{--}\text{C}(=\text{O}21)\text{N}22\text{H}_2$ , act as double donors, and one,  $\text{--}\text{C}(=\text{O}31)\text{N}32\text{H}_2$ , as a single donor and acceptor. The water oxygen  $\text{O}4$  acts as a double acceptor.



Furthermore,  $\pi$ -stacking interactions are also observed in complex 4. There are two distinct interactions of that kind, formed between two identical (two symmetry-equivalent rings N11C12–C16) as well as two different pyridine rings (N11C12–C16 and N31C32–C36), and interestingly only *trans*-related pyridine rings N11C12–C16 and N31C32–C36 are involved (Fig. 4c). Analysis of short ring–ring distances showed that the  $C_g1 \cdots C_g3^i$  distance of 3.9284(2) Å and  $C_g3 \cdots C_g3^{ix}$  distance of 3.9721(2) Å ( $C_g1$  and  $C_g3$  are the centroids of the N11C12–C16 and N31C32–C36 rings, respectively) represent  $\pi$ -stacking interactions (symmetry codes: (i)  $1/2 - x, -1/2 + y, 1/2 - z$ ; (ix)  $1 - x, y, 1/2 - z$ ). In addition, the crystal structure suggests a weak sulphur– $\pi$  interaction between the pyridine ring N21C22–C26 and the S2 atom of the anionic thiocyanate ligand with the  $C_g2 \cdots S2^x$  distance of 3.8829(1) Å (symmetry code: (x)  $1/2 - x, 1/2 - y, -z$ ). Pyridine H atoms are also involved in weak hydrogen bonding interactions C–H $\cdots$ O, C–H $\cdots$ N and C–H $\cdots$ S that further stabilize the structure.

**[Ni(NCS)<sub>2</sub>(isn)<sub>3</sub>(H<sub>2</sub>O)] $\cdot$ 3[Ni(NCS)<sub>2</sub>(isn)<sub>4</sub>] $\cdot$ 9H<sub>2</sub>O (4).** Complex 4 crystallizes in the triclinic space group  $P\bar{1}$ . Each asymmetric unit has four central metal Ni(II) cations showing an octahedral coordination. One nickel (Ni1) cation is coordinated into a discrete octahedral complex unit [Ni1(NCS)<sub>2</sub>(isn)<sub>3</sub>(H<sub>2</sub>O)] by three pyridine (N11, N21, N31) and two thiocyanate (N1, N2) nitrogens and one oxygen (O1) of the coordinated water. The other three nickel(II) cations (Ni2, Ni3, Ni4) also exhibit slightly

distorted NiN<sub>2+4</sub> octahedra, occurring from the coordination of the N atoms of the two terminal thiocyanates and the pyridine N atoms of four isonicotinamides, forming three mutually isolated complex units [Ni(NCS)<sub>2</sub>(isn)<sub>4</sub>] (Fig. 5a). The Ni–N bond lengths to thiocyanates are slightly shorter than those to the pyridine N atoms, which is in line with similar structures (Table 1). The sulphur atoms are involved in N–H $\cdots$ S, O–H $\cdots$ S and C–H $\cdots$ S hydrogen-bonding interactions, which link complex units.

The crystal structure of 4 can be divided into two types of regularly alternating (001) slabs of similar thickness which is about one-half of the 22.3982 Å *c*-axis. Slab I is situated between approximately  $z \approx -0.25$  and  $\approx 0.25$  and slab II between  $z \approx 0.25$  and  $\approx 0.75$  (Fig. 5b and 6a). Each slab shares common Ni coordination octahedra Ni1N<sub>2+3</sub>O, Ni2N<sub>2+4</sub>, Ni3N<sub>2+4</sub> and Ni4N<sub>2+4</sub> with adjacent slabs.

The coordination octahedra situated at two slab boundaries (at  $z \approx 0.25$  and  $z \approx 0.75$ ) are related by symmetry centres. Both slabs host differently oriented isonicotinamide ligands that are almost parallel to the (1 0 2) and (2 0  $\bar{1}$ ) planes in slab I and to the (0 1 1) and (0  $\bar{2}$  1) planes in slab II (Fig. 5b and 6a). Both slabs host thiocyanates as well. Their S atoms are located close to the slab boundaries (Fig. 6b). Additionally, water molecules occupy the voids formed between ligands in both slabs. Slab I includes seven water molecules, one coordinated H<sub>2</sub>O1 and six co-crystallized H<sub>2</sub>O2–H<sub>2</sub>O7.

Middle strong classical O–H $\cdots$ O hydrogen bonds were found between neighbouring hydrogen and oxygen atoms of adjacent H<sub>2</sub>O1–H<sub>2</sub>O4 water molecules at the oxygen–oxygen distance in the range of 2.774–2.869 Å. With one amide

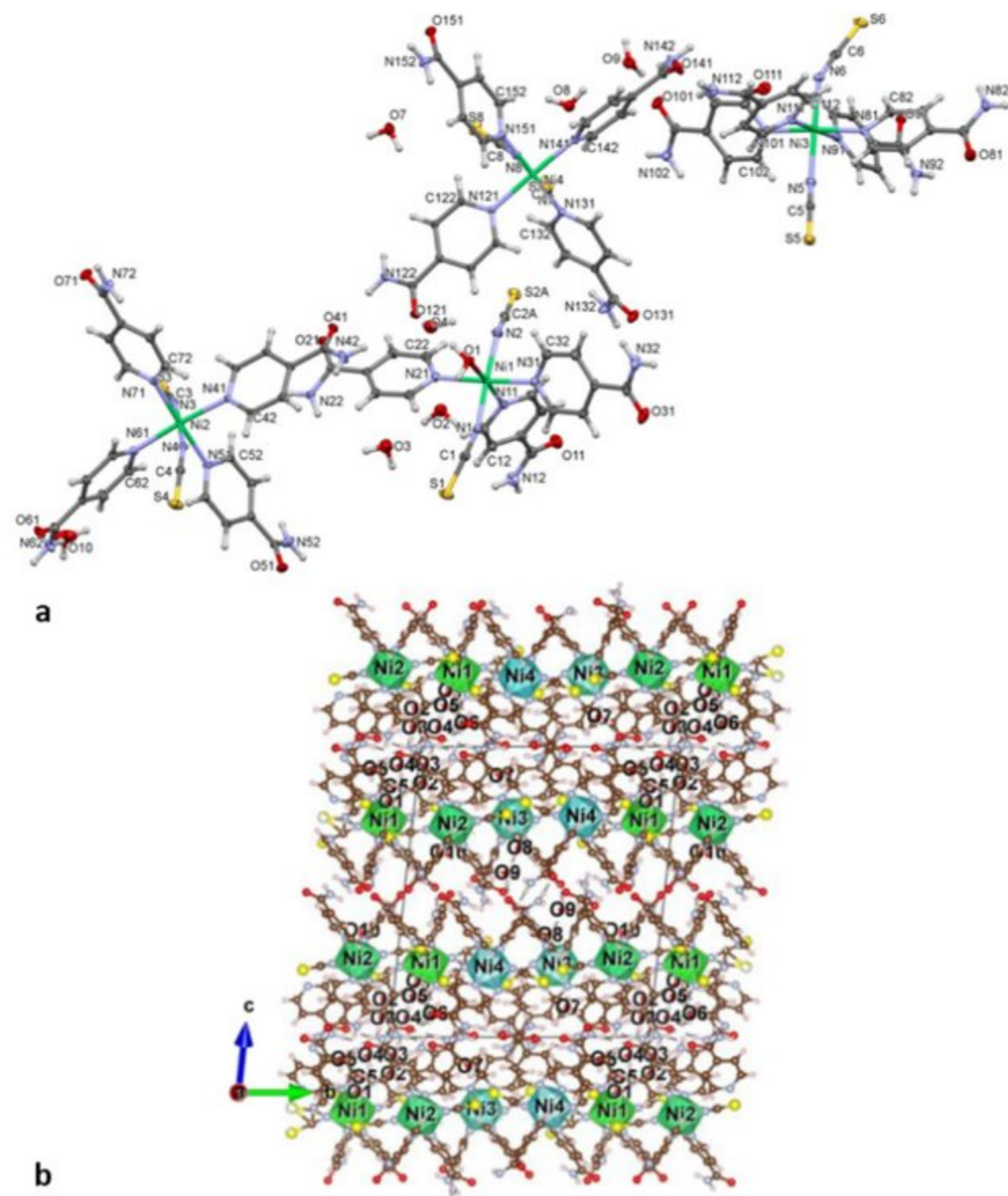


**Fig. 5** Molecular structure of 4 with the atom-numbering scheme. Four complex units and nine co-crystallized H<sub>2</sub>O molecules in the asymmetric unit are shown (a). Crystal packing of 4 viewed down the *a*-axis showing the alternation of two kinds of (001) slabs (oriented horizontal in the figure): slab I is situated between  $z \approx -0.25$  and  $\approx 0.25$  and slab II between  $z \approx 0.25$  and  $\approx 0.75$  (b).

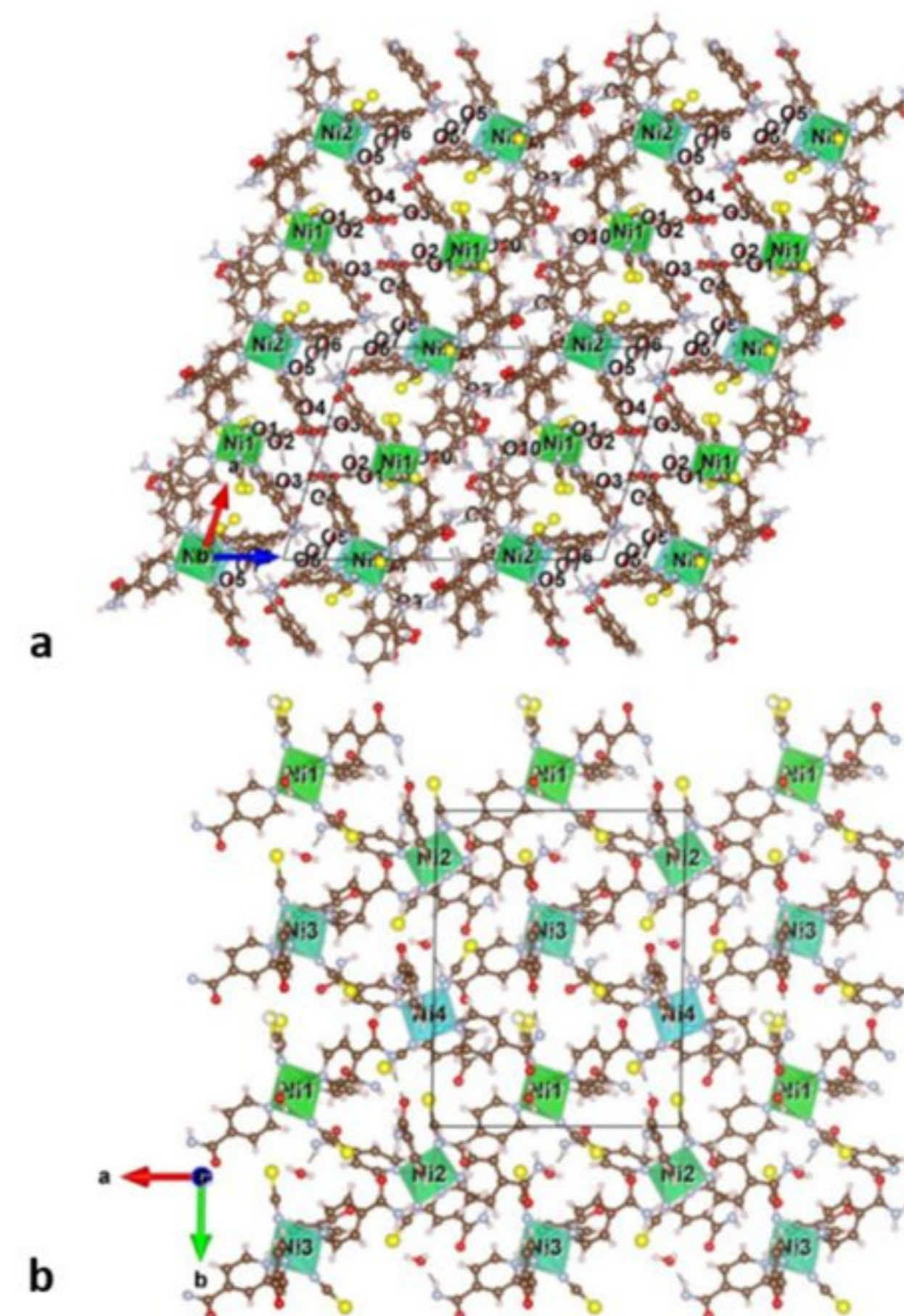


**Fig. 6** The alternating (001) slabs in the crystal structure of 4 projected along [010] (a). The thin layer in the slab boundary at  $z \approx 0.75$  in the crystal structure of 4 projected along [001] (b).

oxygen atom as a double acceptor and their symmetry equivalents, one decamer  $R_{10}^8(20)$  around the inversion centre at 0.5 0 0 was formed (Scheme S2a†).

The water molecules  $H_2O5$  and  $H_2O6$  with amide oxygens and their symmetry equivalents form one hexamer  $R_6^6(16)$  around the centre of symmetry at 0 0 0 in slab I (Scheme S2b†). Decameric and hexameric rings are linked by water  $H_2O5$  which acts as a hydrogen bond donor towards  $H_2O6$  and as a hydrogen bond acceptor towards  $H_2O4$ . Waters  $H_2O7$  are involved in weak intermolecular  $N-H\cdots O$  and  $O-H\cdots S$  hydrogen-bonding interactions. *Via* the amide group,  $H_2O7$  is attached to the hexameric ring  $R_6^6(20)$  formed between the four amide groups and two waters ( $H_2O6$  with its symmetry equivalent) around the inversion centre at 0 0 0 in slab I (Scheme S2c†). Slab II contains only three ( $H_2O8-H_2O10$ ) co-crystallized waters. Two of them ( $H_2O8$  and  $H_2O9$ ) are mutually connected by  $O-H\cdots O$  hydrogen bonds where  $H_2O8$  acts as a donor towards  $H_2O9$ . Four waters ( $H_2O8$  and  $H_2O9$  with their symmetry equivalents) and two amides are involved in the construction of the  $R_6^6(16)$  hexameric ring around the inversion centre at 0 0.5 0.5 (Scheme S3a†). Around the inversion centre at 0.5 0.5 0.5 in slab II, a typical head-to-head amide–amide hydrogen bond  $R_2^2(8)$  dimer in combination with two  $R_4^3(10)$  tetramers are found (Scheme S3b†). Each  $R_4^3(10)$  tetramer is formed between water ( $H_2O9$  with its symmetry equivalent) and three differently acting amides: one serves as both donor and acceptor, whereas the second is a double acceptor and the third is a double donor. Similar to  $H_2O7$  from slab I, waters  $H_2O10$  from slab II are involved in weak  $N-H\cdots O$  and  $O-H\cdots S$  hydrogen bonds, thus linking slabs into a 3D network. Again, the typical head-to-head amide–amide hydrogen bond  $R_2^2(8)$  dimer situated around the inversion centre at 0.5 0 0.5 was found (Scheme S3c†). The structure is further stabilized by the weak intermolecular  $N-H\cdots S$  and  $C-H\cdots S$  hydrogen-bonding interactions (Scheme S3d†).

The centroid–centroid distances between adjacent pyridines, which are equal and greater than 4.6416(1) Å, are probably too long for any  $\pi$ -stacking contacts. The crystal structure suggests six weak sulphur– $\pi$  interactions between pyridine centroids  $C_g$  and S atoms of the anionic thiocyanate with  $S\cdots C_g$  distances from 3.5646(1) to 3.9842(1) Å [3.8004(1), 3.9842(1), 3.7509(1), 3.5646(1), 3.8108(1), 3.9277(1) Å for  $S1-C_g5^i$ ,  $S5-C_g4^{ii}$ ,  $S6-C_g15$ ,  $S7-C_g2$ ,  $S8-C_g9^{iii}$ ,  $S2B-C_g12^{iv}$ , respectively (symmetry codes: (i):  $1-x, -y, 1-z$ , (ii):  $-x, 1-y, 1-z$ , (iii):  $1+x, y, z$ , (iv):  $-1+x, y, z$ ]. In addition, the five  $O\cdots C_g$  distances in the range of 3.3855(1)–3.9790(1) Å suggest a presence of oxygen– $\pi$  bonding interactions between pyridine ring centroids and amide O atoms [3.8561(1), 3.4506(1), 3.3855(1), 3.9790(1), 3.3958(1) Å for  $O71-C_g10^v$ ,  $O91-C_g9^{vi}$ ,  $O111-C_g6^{vii}$ ,  $O131-C_g7^{viii}$ ,  $O151-C_g15^{ix}$ , respectively (symmetry codes: (v):  $-x, 1-y, 1-z$ , (vi):  $1-x, 1-y, -z$ , (vii):  $1-x, 1-y, 1-z$ , (viii):  $1+x, y, z$ , (ix):  $2-x, 1-y, -z$ ].

**[Ni(NCS)<sub>2</sub>(isn)<sub>4</sub>] $\cdot$ 3H<sub>2</sub>O (5).** Complex 5 crystallizes in the orthorhombic space group *Pbcn* with half of the complex molecule in the asymmetric unit since the Ni(II) ion lies on the twofold axis (special position 4c, site symmetry 2). One of

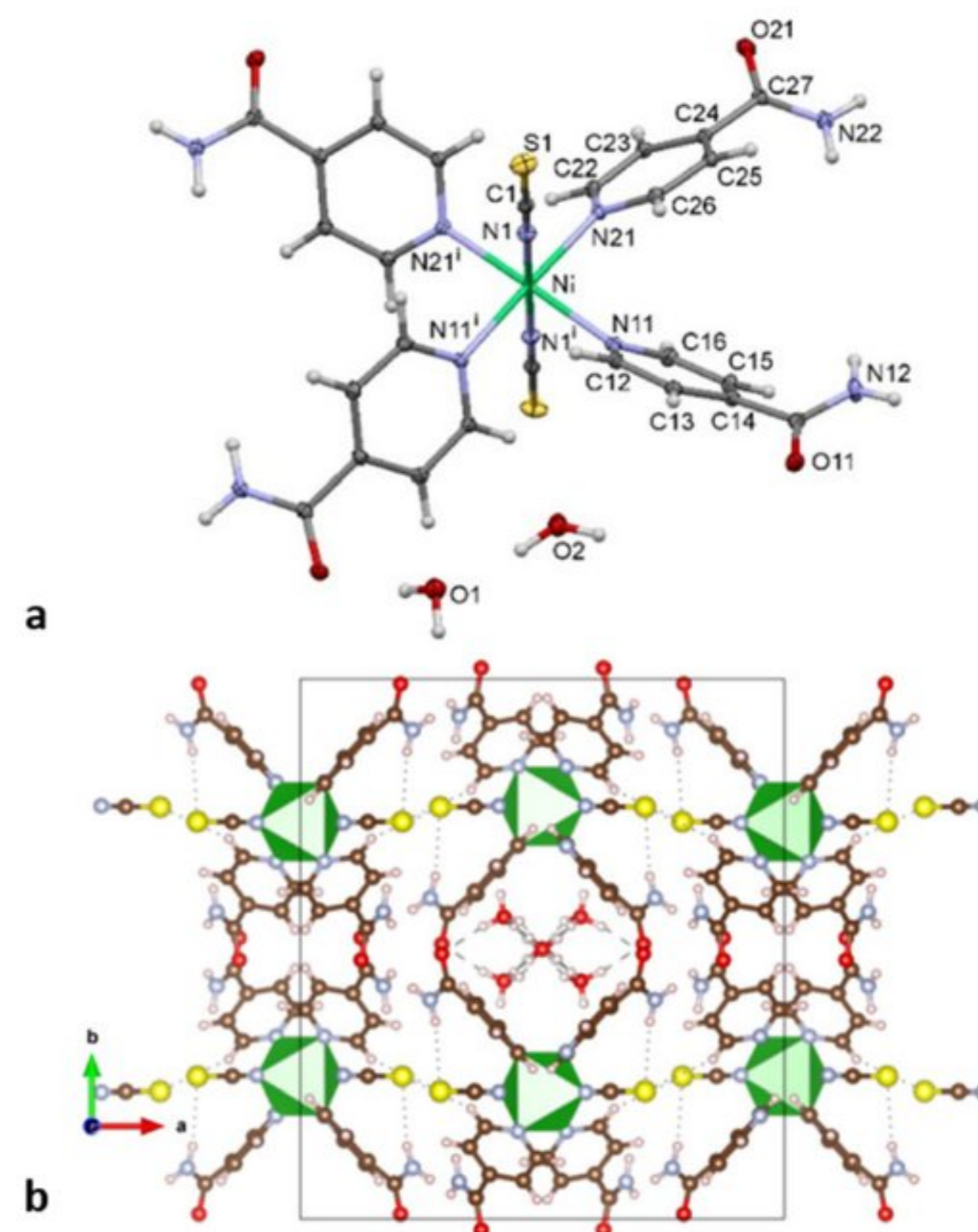


**Fig. 7** Molecular structure of 5 with the atom numbering scheme (symmetry code: (i)  $-x + 1, y, -z + 1/2$ ). Only one pair of the disordered hydrogens on both waters is shown (a). Crystal packing viewed down the *c*-axis showing the hydrogen bond pattern represented by dashed ( $H\cdots O$ ) and dotted ( $H\cdots S$ ) lines (b).

the crystal waters ( $H_2O2$ ) also lies on the twofold axis while the other one ( $H_2O1$ ) is in the general position. Both water molecules O1 and O2 show H-atom positional disorder and have partial-occupancy H atoms: H1A and H1C have occupancies of 0.5, while H1B is fully occupied. H2A and H2B have 0.5 occupancies and form a distorted tetrahedron since O2 lies on a twofold axis. Since H1A and H2A point toward each other, either one or the other is present at each site. The central Ni(II) and its attached ligands form a slightly distorted octahedron. The molecular structure is shown in Fig. 7, and the geometrical parameters are in Tables 1 and S3–S5.† An extensive hydrogen bonding framework interlinks the complex and water molecules into a 3D supramolecular framework. One amide  $N-H$  donor is involved in hydrogen bonding of the type  $N-H\cdots O$  toward an amide oxygen atom of an adjacent molecule and the other one of the type  $N-H\cdots S$  toward S atoms of the adjacent thiocyanate group. One complex molecule is linked to eight neighbouring complex molecules by these hydrogen bonds. Water molecules are mutually interlinked by hydrogen bonds and one ( $H_2O1$ ) additionally acts as a donor toward an amide oxygen (O11) atom. Each water molecule donates two hydrogen atoms to form hydrogen bonds with two other water molecules ( $A\cdots D$  distances are 2.8109(15) and 2.8525(16) Å) and accepts two hydrogen bonds from two more water molecules, forming  $R_4^2(8)$  tetramers (Scheme S1c†). In that way hydrogen atoms form bridges to the oxygen atoms of adjacent water molecules. Similar bridges between thiocyanate S and nitrogen atoms of adjacent carboxamide groups are also formed (Scheme S1b†).

As mentioned, the carboxamide O11 oxygen additionally accepts a water hydrogen atom ( $A\cdots D$  distance is 2.8715(15) Å). Sharing one common water molecule,  $R_4^2(8)$  cyclic water tetramers are linked in the zigzag hydrogen bonded chains running parallel to the  $c$ -axis. The adjacent  $R_4^2(8)$  tetramers in the chain do not lie in the same plane but are rotated by  $90^\circ$  relative to each other (Scheme S4a†). Other parallel infinite  $C(4)$  hydrogen bond chains (Scheme S4b†) were formed by including the carboxamide oxygens O11 and O22. They accept amide hydrogen atoms from neighbouring molecules and form the  $N-H\cdots O$  type of interactions with  $A\cdots D$  distances of 3.1408(16) and 2.9909(16) Å. These  $C(4)$  hydrogen bond chains are connected by additional intermolecular interactions of the  $N-H\cdots S$  type ( $A\cdots D$  distances are 3.6598(13) and 3.4981(13) Å), where the thiocyanato S1 atom acts as a bifurcated hydrogen bond acceptor for two  $N-H\cdots S$  hydrogen bonds. In that way,  $R_8^6(24)$  rings are formed by carboxamide groups  $-C(=O)NH_2$  and the thiocyanato S1 atom of adjacent molecules by the interactions of  $N-H\cdots O$  and  $N-H\cdots S$  types (Scheme S4c†). Also, the thiocyanato S1 atom acts as a hydrogen bond acceptor for weak hydrogen bonding interactions of the  $C-H\cdots S$  type ( $A\cdots D$  distances are 3.6436(13) Å). These  $C-H\cdots S$  hydrogen bonding interactions are connected, forming two fused  $R_3^2(12)$  and  $R_2^2(16)$  rings (Scheme S4d†). The shortest centroid-centroid distance of 4.6911(1) Å between adjacent pyridine rings is probably too long for any  $\pi$ -stacking interactions. The  $O22\cdots C_{g2}^{viii}$  distance of 3.1140(1) Å indicates a possible weak oxygen- $\pi$  bonding interaction (symmetry code: (viii)  $x, 1 - y, -1/2 + z$ ).

**[Ni(NCS)<sub>2</sub>(isn)<sub>4</sub>] $\cdot$ 2(isn) (6).** The structure of isonicotinamide complex **6** is very similar to that of the cobalt N-bonded SCN-complex  $[Co(NCS)_2(isn)_4]\cdot 2isn\cdot EtOH$ ,<sup>21</sup> having the same triclinic centrosymmetric space group, similar lengths of unit cell axis and a slightly different chemical composition: besides the different metal ion, the structure of **6** does not contain ethanol solvent molecules. The central metal ions Ni(II) are coordinated by six N atoms, four from isonicotinamides in equatorial and two from terminal bonded thiocyanates in axial positions (Fig. 8a). Bond lengths illustrate a low octahedral distortion of  $NiN_{4+2}$  octahedra (Tables 1 and S3–S5†). The complex units  $[Ni(NCS)_2(isn)_4]$  and two isonicotinamide solvent molecules are connected by various types of interactions:  $N-H\cdots O$ ,  $N-H\cdots S$ ,  $N-H\cdots N$ ,  $C-H\cdots O$  and  $C-H\cdots S$ . The carboxamide groups  $-C(=O21)N22H_2$  and  $-C(=O31)N32H_2$  of two isonicotinamide ligands form  $C(4)$  hydrogen bond chains in the  $[100]$  direction (Scheme S5†). Both amide nitrogens N22 and N32 act as hydrogen bond donors in one additional interaction of the  $N-H\cdots N$  type ( $A\cdots D$  distances are 2.9216(19) and 2.9222(19) Å) that links  $C(4)$  hydrogen bond chains with pyridine ring nitrogens of the isonicotinamide solvent molecules. The same two isonicotinamide ligands form two types of parallel and vacant channels (Fig. 8b). Both channels run along the  $a$ -axis and are located at the positions  $(a, 0, 0)$  and  $(a, 1/2, 0)$ , respectively. The  $C(4)$  hydrogen bond

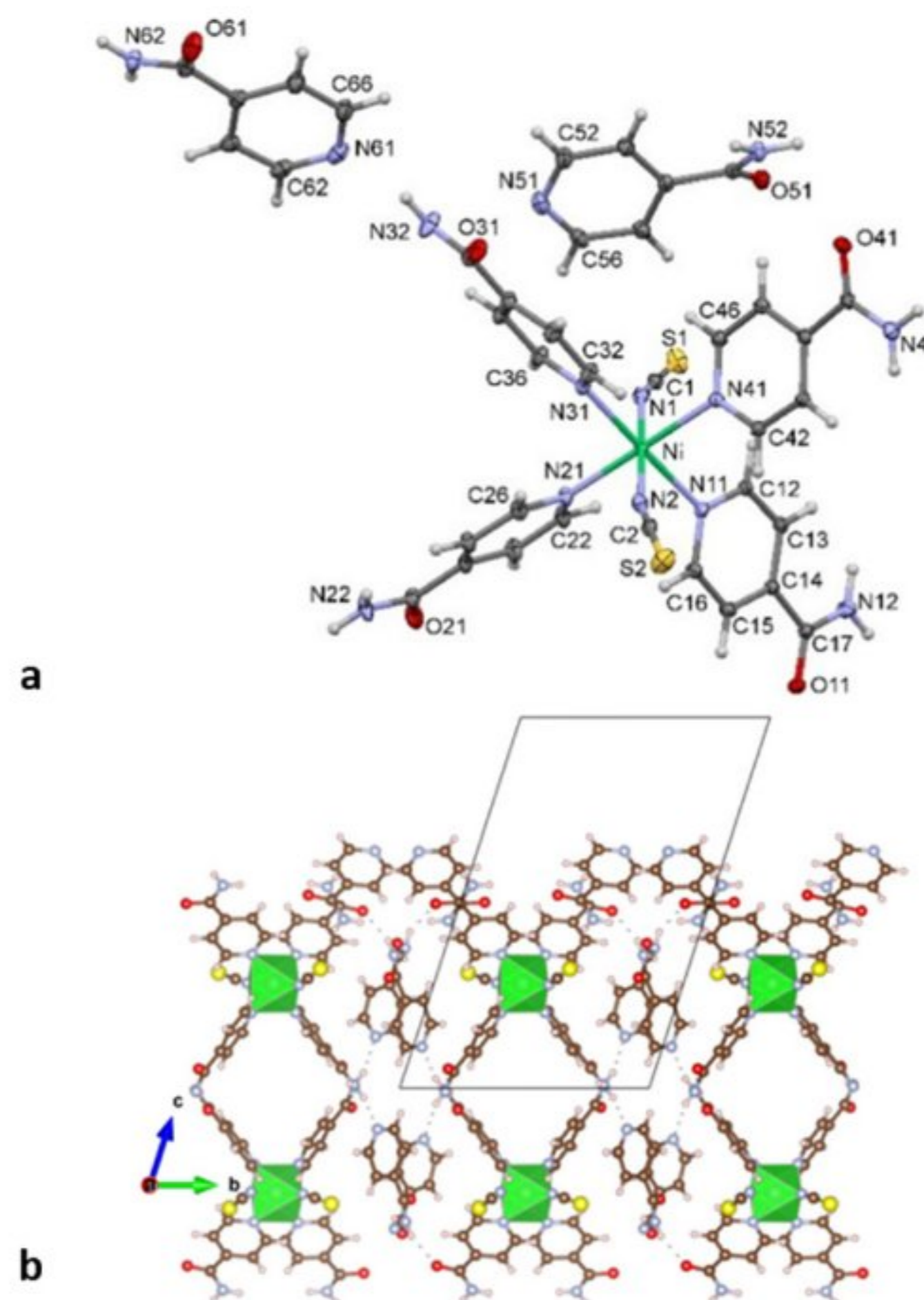


**Fig. 8** Molecular structure of **6** with the atom-numbering scheme (a). Crystal packing of **6** viewed down the  $a$ -axis showing the hydrogen bond pattern represented by dashed ( $H\cdots O$ ) and dotted ( $H\cdots N$  and  $H\cdots S$ ) lines (b).

chains formed by the carboxamide groups,  $-C(=O21)N22H_2$  and  $-C(=O31)N32H_2$ , and pyridine ring nitrogen atoms of isonicotinamide are positioned on the walls of the smaller channel 1, while two  $NiN_{4+2}$  octahedra and two pairs of centrosymmetrically related isonicotinamide ligands are situated on the walls of the larger channel 2.

Channel 2 in **6** is practically empty because the highest peak in the final difference map is just  $0.26 e \text{ \AA}^{-3}$  and the electron density could not be reasonably modelled. In similar channels in  $[M(NCS)_2(isn)_4]\cdot 2(isn)\cdot EtOH$ ,  $M = Co^{21}$  or  $Ni$ ,<sup>23</sup> ethanol solvent molecules were found. Two other carboxamides  $-C(=O51)N52H_2$  and  $-C(=O61)N62H_2$  of the co-crystallized isonicotinamides form similar  $C(4)$  hydrogen bond chains in the same  $[100]$  direction. They are linked by  $N-H\cdots O$  ( $A\cdots D$  distances are 2.7756(17), 2.8472(16), 2.8940(17), 2.9096(17) Å) contacts to carboxamides  $-C(=O11)N12H_2$  and  $-C(=O41)N42H_2$  of coordinated isonicotinamide ligands, thereby forming a 2D corrugated sheet network in the  $(002)$  planes with a combination of  $R_4^4(16)$ ,  $R_4^4(16)$ ,  $R_4^4(24)$  and  $R_8^6(24)$  graph-set motifs (Scheme S5†). Sulphur atoms belonging to terminal SCN ligands participate in weak  $C-H\cdots S$  interactions. Weak  $C-H\cdots O$  interactions are also present.

The analysis of short ring-ring distances showed that the  $C_{g5}\cdots C_{g6}$  distance of 3.5945(1) Å represents  $\pi$ -stacking interactions and that the  $C_{g2}\cdots C_{g6}^{vi}$  distance of 4.1756(1) Å (symmetry code: (vi):  $x, -1 + y, z$ ) can be a weak  $\pi$ -stacking interaction, while all other  $C_g\cdots C_g$  distances between adjacent pyridine rings, which are equal and greater than 4.6103(1) Å, are probably too long for any  $\pi$ -stacking

interactions. Among the investigated complexes, the shortest  $S1 \cdots C_g4^{vi}$  distance of 3.6985(1) Å has been found between the adjacent molecules in **6**. In addition, the  $O11 \cdots C_g1^{vii}$  distance of 3.5527(1) and  $O41 \cdots C_g4^{viii}$  distance of 3.9705(1) Å suggest the presence of oxygen- $\pi$  bonding interactions (symmetry codes: (vi)  $1 + x, y, z$ , (vii)  $1 - x, -y, 1 - z$ , (viii)  $-x, 1 - y, 1 - z$ ).

$[Ni(NCS)_2(isn)_4] \cdot 1.25H_2O$  (**7**). There were not enough crystals for other analyses except X-ray. Since the structure was solved just before sending the manuscript all data are presented in Discussion S2 and Fig. S3–S5.†

### NMR spectroscopy

The  $^1H$  NMR proton spectra in  $DMF-d_7$  show one set of signals, except for **6**, where the free isonicotinamide H-2/6 signal was observed at 8.75 ppm, being in accordance with its crystal structure (Fig. 9). Coordination of the Ni(II) ion to the lone pair of electrons of the pyridine ring nitrogen was confirmed by two very broad singlets observed in a low magnetic field due to paramagnetism. The *ortho*-protons (H-2/6) in the  $^1H$  spectra of **1–3**, **5**, and **6** appeared as the most downfield shifted signals, in the range of 114–120 ppm ( $\Delta\nu_{1/2} = 7000–9000$  Hz). The *meta*-protons (H-3/5) appeared at about 40 ppm ( $\Delta\nu_{1/2} = 1500–2000$  Hz). The chemical shift and line width of the signals are consistent with the length of the chemical bond in the crystal (Table 2).<sup>44</sup> The signals of the amide protons were sharpest in the  $^1H$  spectra (marked with a square in Fig. 9) and with the chemical shifts similar to that in the free ligand.

### Thermogravimetric analysis

The thermal stability of **1–6** was investigated by thermogravimetric analysis. Calculated and theoretical values of the water:nickel ratio as well as decomposition temperatures are given in Table S6.† All four compounds containing crystallization water molecules (**1**, **3**, **4** and **5**) lose

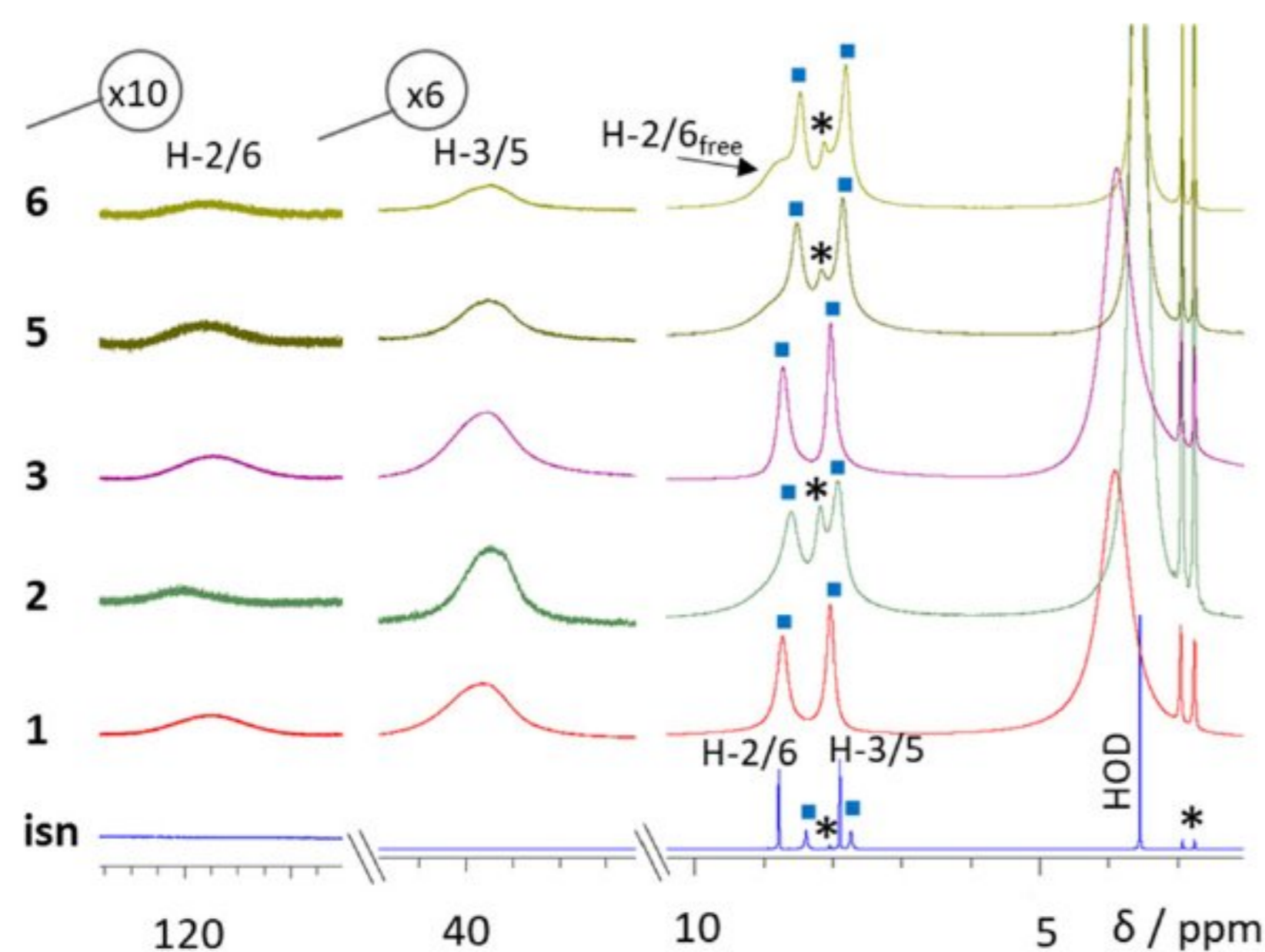


**Fig. 9** 500 MHz (**1**) and 600 MHz proton NMR spectra of the ligand (*isn*) and its nickel(II) complexes (**2**, **3**, **5**, and **6**) in  $DMF-d_7$ . The intensity in the downfield region of the spectra is multiplied by six or ten. The asterisks mark the residual solvent signals. The squares mark  $NH_2$  proton signals.

**Table 2** NMR parameters in  $DMF-d_7$  at 298 K and crystal structure data for complexes **1–3**, **5** and **6**

Complex	Atoms	$\delta$ (ppm)	$\Delta\nu_{1/2}^a$ (Hz)	$Ni \cdots H^b$ (Å)
<b>1</b>	H-2/6	114.3	7986	3.05
	H-3/5	38.7	1500	5.06
<b>2</b>	H-2/6	120.1	6800	3.05
	H-3/5	38.9	1596	5.06
<b>3</b>	H-2/6	114.3	7996	3.07
	H-3/5	39.2	1920	5.07
<b>5</b>	H-2/6	116.5	8986	3.05
	H-3/5	39.1	1584	5.06
<b>6</b>	H-2/6	116.4	8908	3.06
	H-3/5	39.0	1584	5.07

<sup>a</sup> Signal half-widths were read at half of the signal height. <sup>b</sup> The mean value of all distances observed between the H atoms and the metal ion in the crystal.

water at significantly lower temperatures (**1** at 67 °C; **3** at 50 °C; **4** at 42 °C; **5** at 45 °C) than **2** (at 105 °C), which contains only coordinated water molecules. The stability of dehydrated complexes is correlated with the number of coordinated isonicotinamides. Compounds with fewer *isn* ligands decompose at higher temperatures (dehydrated **2** decomposes at 190 °C) and *vice versa* (**6** decomposes at 160 °C). All compounds have similar decomposition mechanisms with several successive steps starting with *isn* elimination (Fig. S6†). Complexes **2–6** completely decompose to nickel(II) oxide in the temperature range 740–805 °C.

### Infrared spectroscopy

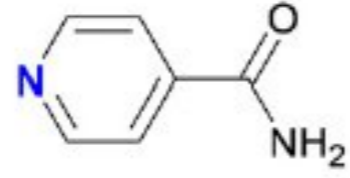
The IR data for compounds **1–6** are given in Fig. S7.1–S7.6.† The position of the C–N stretching frequencies in the IR spectra of all complexes is observed at higher values in comparison with this band of the free  $SCN^-$  ligand and does not corroborate with the reported data so far<sup>45,46</sup> (neither for the M–NCS nor for the M–SCN coordinated mode). The position of the C–S stretching frequencies follows the usual values as well as  $\delta(SCN)$ . CO stretching frequencies are shifted to slightly higher frequencies due to combined inductive effect and resonance.

### Density functional theory calculations

DFT calculations were employed to offer more insight into fundamental features of the studied ligands and to provide molecular interpretation to the observed differences in the crystal structures of their metal complexes. Initially, we considered 1:1 Ni(II):ligand complexes (Table 3) in order to evaluate intrinsic ligand tendencies towards nickel.

Water is the simplest ligand and its only nucleophilic site, the O atom, bears the largest single-site amount of negative charge among ligands,  $q(O) = -1.05 |e|$ . Still, Ni(II) forms the least stable complex with water, which is by 4–5 kcal mol<sup>-1</sup> surpassed by the other two ligands. Through the Pearson HSAB principle, this clearly illustrates the preference of Ni(II) towards soft bases such as *isn* and thiocyanate over hard

**Table 3** Calculated bond distances (in Å), NBO atomic charges (in |e|) and interaction free energies ( $\Delta G_{\text{INT}}$ , in kcal mol<sup>-1</sup>) for 1:1 Ni(II):ligand complexes with the (SMD)/ $\omega$ B97X-D/LANL2DZ model. The ligand coordinating atom is given in blue

Ligand		SCN <sup>-</sup>	H <sub>2</sub> O
Atomic charges	$q(\text{N})$	-0.54	-0.63
	$q(\text{O/S})$	-0.75	-0.43
	$q(\text{ring})$	-1.02	
Ni <sup>2+</sup>	$q(\text{Ni}^{2+})$	1.84	1.90
	Ni-N/O	1.96	1.92
	$\Delta G_{\text{INT}}$	-72.9	-67.7

bases such as water, despite the much higher nucleophilicity of the latter. More importantly, it also justifies why only up to two water ligands are present in the final structures, whose existence in the first coordination sphere does not maximize metal-ligand interactions but rather serves the role of intermolecularly connecting monomers into the final 3D crystal structures, where water's ability to undergo hydrogen bonding plays a dominant part. This notion also confirms that the availability of isn and SCN<sup>-</sup> ligands will lead to their exchange with water for the metal binding from the initial [Ni(H<sub>2</sub>O)<sub>6</sub>]<sup>2+</sup> complexes.

All Ni(II) complexes are characterized with high exergonicities (Table 3), tying in with similar reports in the literature.<sup>47</sup> This is, at least partly, explained by a large electrostatic character of the formed complexes, being evident in a high charge transfer among interacting partners, between 0.10 and as much as 0.16 |e| (Table 3). In line with that, Ni(II) forms the least stable 1:1 complex with neutral water,  $\Delta G_{\text{INT}} = -67.7$  kcal mol<sup>-1</sup>, and accepts the least charge from that ligand. On the other hand, thiocyanate is an anionic ligand, but the excess negative charge is resonantly dispersed among N and S atoms (Table 3) allowing both sites to act as Lewis bases. Yet, its N atom accumulates more negative charge (-0.63 |e| vs. -0.43 |e| on oxygen), which rationalizes why Ni(II)-thiocyanate complexes are formed through metal-N bonds, which outperforms the Ni(II)-water complex ( $\Delta G_{\text{INT}} = -71.9$  kcal mol<sup>-1</sup>). Interestingly, isonicotinamide shows the highest ability to bind Ni(II) at

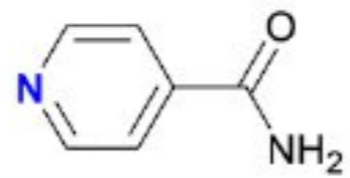
$\Delta G_{\text{INT}} = -72.9$  kcal mol<sup>-1</sup>, which is again established with the nitrogen donor from the pyridine ring. In contrast, the corresponding analogues with Ni-O(amide) and Ni-S(thiocyanate) bonds are by 6.2 and 15.9 kcal mol<sup>-1</sup> less stable. The observed trends in the stability of 1:1 complexes, isn > SCN<sup>-</sup> > H<sub>2</sub>O for Ni(II), already provide some evidence in support of different stoichiometries in the final crystal structures.

Our computational strategy in interpreting the formation of different metal complexes in solution is based on using SCN<sup>-</sup> and isn ligands to sequentially replace waters from the initial [Ni(H<sub>2</sub>O)<sub>6</sub>]<sup>2+</sup> complex, formed after dissolving a metal salt in the aqueous solution (Table 4). The latter features a regular octahedral orientation with all Ni-O distances at 2.06 Å (Fig. S8†) and the calculated stability of  $\Delta G_{\text{INT}} = -123.5$  kcal mol<sup>-1</sup>, which will serve as a reference point for other complexes. Also, knowing that the latter value is almost doubled from that calculated for the matching 1:1 Ni(II):water complex, it confirms the hexaaqua complex as the predominant form in the pure aqueous solution.

Unlike the situation with simple 1:1 complexes, where isn turned out as the most efficient in binding Ni(II), in [Ni(H<sub>2</sub>O)<sub>6</sub>]<sup>2+</sup> the first water molecule is most favourably replaced by SCN<sup>-</sup>, thereby offering [Ni(H<sub>2</sub>O)<sub>5</sub>(NCS)]<sup>+</sup>, most likely due to steric reasons. This increases the overall stability to  $\Delta G_{\text{INT}} = -129.8$  kcal mol<sup>-1</sup>, surpassing that of [Ni(H<sub>2</sub>O)<sub>5</sub>(isn)]<sup>2+</sup> by as much as 6.3 kcal mol<sup>-1</sup>, which facilitates the ligand exchange. Interestingly, the stability of [Ni(H<sub>2</sub>O)<sub>5</sub>(isn)]<sup>2+</sup> precisely matches that from the initial [Ni(H<sub>2</sub>O)<sub>6</sub>]<sup>2+</sup> complex, therefore additionally eliminating this substitution route as likely. The same trend is maintained in the tetraaqua complex, where the stability of [Ni(H<sub>2</sub>O)<sub>4</sub>(NCS)<sub>2</sub>] is further increased to  $\Delta G_{\text{INT}} = -135.3$  kcal mol<sup>-1</sup>, while an analogous [Ni(H<sub>2</sub>O)<sub>4</sub>(NCS)(isn)]<sup>+</sup> is unstable and decomposes during the geometry optimization. It is worth noting that in [Ni(H<sub>2</sub>O)<sub>4</sub>(NCS)<sub>2</sub>], the two inserted thiocyanate ligands are most favourably located in a *trans* position (Fig. S8†), which is maintained throughout the remaining subsequent complexes. The latter is found in excellent agreement with experimental data, where this was the case in all complexes.

Interestingly, the third water is most favourably replaced by the isn ligand, as in [Ni(H<sub>2</sub>O)<sub>3</sub>(NCS)<sub>2</sub>(isn)] ( $\Delta G_{\text{INT}} = -141.5$

**Table 4** Calculated interaction free energies ( $\Delta G_{\text{INT}}$ , in kcal mol<sup>-1</sup>) for various complexes during the sequential exchange of water molecules with isn and SCN<sup>-</sup> ligands obtained at the (SMD)/ $\omega$ B97X-D/LANL2DZ level of theory. The ligand coordinating atom is given in blue. Interaction free energies for complexes with experimentally determined crystal structures are given in bold

Ligand		SCN <sup>-</sup>
Isolated [Ni(H <sub>2</sub> O) <sub>6</sub> ] <sup>2+</sup>	-123.5	
[Ni(H <sub>2</sub> O) <sub>6</sub> ] <sup>2+</sup>	[Ni(H <sub>2</sub> O) <sub>5</sub> (isn)] <sup>2+</sup>	-123.5
[Ni(H <sub>2</sub> O) <sub>5</sub> (NCS)] <sup>+</sup>	[Ni(H <sub>2</sub> O) <sub>4</sub> (NCS)(isn)] <sup>+</sup>	Not stable
[Ni(H <sub>2</sub> O) <sub>4</sub> (NCS) <sub>2</sub> ]	[Ni(H <sub>2</sub> O) <sub>3</sub> (NCS) <sub>2</sub> (isn)]	-141.5
[Ni(H <sub>2</sub> O) <sub>3</sub> (NCS) <sub>2</sub> (isn)]	[Ni(H <sub>2</sub> O) <sub>2</sub> (NCS) <sub>2</sub> (isn) <sub>2</sub> ]	<b>-145.4</b>
[Ni(H <sub>2</sub> O) <sub>2</sub> (NCS) <sub>2</sub> (isn) <sub>2</sub> ]	[Ni(H <sub>2</sub> O)(NCS) <sub>2</sub> (isn) <sub>3</sub> ]	<b>-151.6</b>
[Ni(H <sub>2</sub> O)(NCS) <sub>2</sub> (isn) <sub>3</sub> ]	[Ni(NCS) <sub>2</sub> (isn) <sub>4</sub> ]	<b>-156.9</b>
		[Ni(H <sub>2</sub> O) <sub>5</sub> (NCS)] <sup>+</sup>
		[Ni(H <sub>2</sub> O) <sub>4</sub> (NCS) <sub>2</sub> ]
		[Ni(H <sub>2</sub> O) <sub>3</sub> (NCS) <sub>3</sub> ] <sup>-</sup>
		[Ni(H <sub>2</sub> O) <sub>2</sub> (NCS) <sub>3</sub> (isn)] <sup>-</sup>
		[Ni(H <sub>2</sub> O)(NCS) <sub>3</sub> (isn) <sub>2</sub> ] <sup>-</sup>
		[Ni(NCS) <sub>3</sub> (isn) <sub>3</sub> ] <sup>-</sup>

kcal mol<sup>-1</sup>), which is here able to capitalize on its largest intrinsic affinity for Ni(II) over unfavourable steric requirements, thus leading to a system that is by 2.1 kcal mol<sup>-1</sup> more stable than [Ni(H<sub>2</sub>O)<sub>3</sub>(NCS)<sub>3</sub>]<sup>-</sup>. This complex anchors as a key turning point, after which any further substitution of the remaining water ligands leads to complexes observed experimentally. In this context, from [Ni(H<sub>2</sub>O)<sub>3</sub>(NCS)<sub>2</sub>(isn)], the fourth water is almost equally well replaced by both SCN<sup>-</sup> and isn, differing by only 0.1 kcal mol<sup>-1</sup> in the resulting complex stability. Yet, the stability of [Ni(H<sub>2</sub>O)<sub>2</sub>(NCS)<sub>2</sub>(isn)<sub>2</sub>] prevails and confirms the experimentally observed structures **1** and **2** ( $\Delta G_{\text{INT}} = -145.4$  kcal mol<sup>-1</sup>), while a slightly less stable [Ni(H<sub>2</sub>O)<sub>2</sub>(NCS)<sub>3</sub>(isn)]<sup>-</sup> complex was not isolated from the solution, which puts both sets of results in good agreement. Nevertheless, given a comparable stability of both diaqua complexes, we considered both structures for the substitution of the fifth water molecule. This led to three cases, [Ni(H<sub>2</sub>O)(NCS)<sub>3</sub>(isn)<sub>2</sub>]<sup>-</sup>, [Ni(H<sub>2</sub>O)(NCS)<sub>2</sub>(isn)<sub>3</sub>] and [Ni(H<sub>2</sub>O)(NCS)<sub>4</sub>(isn)]<sup>2-</sup>, whose  $\Delta G_{\text{INT}}$  values are -151.4, -151.6 and -148.6 kcal mol<sup>-1</sup>, respectively. The two structures with the lowest stability were not isolated during experiments, while the highest stability of [Ni(H<sub>2</sub>O)(NCS)<sub>2</sub>(isn)<sub>3</sub>] again places our results in good agreement with experiments and confirms the feasibility of crystal structures **3** and **4**. From there, the last water molecule is most exergonically replaced by another isn ligand, offering the final non-water complex [Ni(NCS)<sub>2</sub>(isn)<sub>4</sub>] with the largest stability of  $\Delta G_{\text{INT}} = -156.9$  kcal mol<sup>-1</sup>, being 1.0 kcal mol<sup>-1</sup> higher than that of analogous [Ni(NCS)<sub>3</sub>(isn)<sub>3</sub>]<sup>-</sup>, which precisely ties in with the experimentally determined structures **5**–**7**.

In concluding this section, let us emphasize that our computational strategy turned useful in rationalizing experimentally isolated complexes whose formation is strongly facilitated thermodynamically. In other words, starting from the hexaaqua complex [Ni(H<sub>2</sub>O)<sub>6</sub>]<sup>2+</sup>, formed upon dissolving the nickel salt in water, every sequential replacement of water ligands leads to more stable complexes, which justifies their formation. This is further supported by the fact that water intrinsically forms the weakest interactions with Ni(II). On the other hand, isn most strongly binds to Ni(II), yet this is experimentally manifested only after the first two water ligands are replaced by SCN<sup>-</sup>, due to its lower steric requirements. Following that, from [Ni(H<sub>2</sub>O)<sub>4</sub>(NCS)<sub>2</sub>], the remaining four waters are most favourably replaced by isn, leading to systems [Ni(H<sub>2</sub>O)<sub>3</sub>(NCS)<sub>2</sub>(isn)], [Ni(H<sub>2</sub>O)<sub>2</sub>(NCS)<sub>2</sub>(isn)<sub>2</sub>], [Ni(H<sub>2</sub>O)(NCS)<sub>2</sub>(isn)<sub>3</sub>] and [Ni(NCS)<sub>2</sub>(isn)<sub>4</sub>], which confirm the experimentally characterized systems **1**–**7**.

The reason for the isolation of complexes bearing one and two water ligands lies in their ability to form hydrogen bonding contacts between monomers in the crystal packing, which then overcomes a slightly lower stability of the elemental octahedral unit. To confirm that, we performed a series of DFT calculations on model monocoordinated complexes Ni–X (X = H<sub>2</sub>O, isn, SCN<sup>-</sup>) and evaluated the

**Table 5** Calculated interaction free energies ( $\Delta G_{\text{INT}}$ , in kcal mol<sup>-1</sup>) among model monocoordinated complexes Ni–X (X = H<sub>2</sub>O, isn, SCN<sup>-</sup>) in Ni–X<sup>1</sup>...X<sup>2</sup>–Ni dimers as obtained with the (SMD)/ $\omega$ B97X-D/LANL2DZ model

X <sup>1</sup> , X <sup>2</sup>	H <sub>2</sub> O	isn	SCN <sup>-</sup>
H <sub>2</sub> O	-97.4	-50.9	-51.3
isn		+6.3	+3.7
SCN <sup>-</sup>			-2.3

interaction energy between the most stable Ni–X...X–Ni dimers (Table 5). The results revealed a clear dominance of water molecules, whose ability to both donate and accept hydrogen bonding largely outperforms other ligands that even tend to offer endergonic combinations among themselves, which agrees with crystallographic data presented here. In addition, we supplemented these results by a detailed analysis of the intermolecular interactions among crystal structures through Hirshfeld surface analysis and thereof derived 2D fingerprint plots (Fig. S9–S17†) and enrichment ratios (*E*) of the corresponding contacts (Tables S7–S9†), which is presented and discussed in Discussion S3.†

## Conclusions

For the synthesis of this type of coordination compounds, the crystallization screening with the isonicotinamide concentration variation was found to be the best method. Yet, scaling up was not always successful since the nucleation depended on the volume of the crystallization solution, type and intensity of mixing, material of the vessel, and probably other factors as well. In this way crystals of **2**–**7** were obtained, often crystallizing in mixtures but were also obtained pure. After the initial crystallization of **1**, it could not be synthesised again, probably being a metastable hydrate of **2**. Among all investigated complexes, an octahedral distortion is observed with two Ni–N<sub>NCS</sub> bonds being slightly shorter than those of Ni–O<sub>w</sub> and Ni–N<sub>isn</sub>. Intermolecular connectivity was thoroughly analysed. It is interesting that, except in **2**–**4**, there is a lack of self-complementary amide–amide dimeric synthon R<sub>2</sub><sup>2</sup>(8). Instead, R<sub>6</sub><sup>4</sup>(12) hexamers and centrosymmetric R<sub>6</sub><sup>4</sup>(16) rings in **1** as well as the carboxamide catemeric C(4) chains in **5** and **6** are found. The complex ring patterns of hydrogen bonding (graph-set descriptors R<sub>4</sub><sup>2</sup>(8), R<sub>2</sub><sup>2</sup>(10), R<sub>4</sub><sup>3</sup>(14) and R<sub>10</sub><sup>6</sup>(24)) were observed in **3**, while R<sub>10</sub><sup>8</sup>(20) decamers, R<sub>6</sub><sup>4</sup>(14), R<sub>6</sub><sup>6</sup>(16), R<sub>6</sub><sup>6</sup>(20) hexamers and R<sub>4</sub><sup>3</sup>(10) tetramers were found in **4**.

The adjacent pyridine rings are interlinked by the  $\pi$ -stacking interactions in **2**, **3** and **6**. Sulphurs from the terminal SCN<sup>-</sup> and isonicotinamide amide oxygens are observed in a close contact (<4.0 Å) with the aromatic pyridine rings in **3**–**6**. Oxygen– $\pi$  bonding interactions between pyridine ring centroids and amide oxygens were found in **4** and **6**. The amide nitrogen atoms do not participate in the coordination but only form weak N–H...O, N–H...N and N–H...S hydrogen bonding interactions.

Pyridine H atoms are also involved in weak hydrogen bonding interactions of the C–H...X type (X = O, N, S).

Computational analysis revealed that the employed ligands exhibit different affinities towards Ni(II),  $\text{isn} > \text{SCN}^- > \text{H}_2\text{O}$ , which leads to dissimilar stoichiometries in the determined crystal structures. Given a much lower affinity of water, the presence of these ligands in the final complexes is afforded by water's ability to connect discrete monomeric complexes through hydrogen bonding interactions into the crystal packing rather than from offering the most stable octahedral units.

## Author contributions

The manuscript was written through contributions of all authors. All authors have given approval to the final version of the manuscript.

## Conflicts of interest

There are no conflicts to declare.

## Acknowledgements

This research was financially supported by the Ministry of Science, Education and Sports of the Republic of Croatia Grants No. 119-1193079-1332, the Croatian Science Foundation (IP-2020-02-8090) and grants from the University of Zagreb for 2020 and 2021. L. H. wishes to thank the Croatian Science Foundation for a doctoral stipend through the Career Development Project for Young Researchers (DOK-2020-01-3482). L. H. and R. V. would like to thank the Zagreb University Computing Centre (SRCE) for granting computational resources on the ISABELLA cluster. We acknowledge the support of project CIuK co-financed by the Croatian Government and the European Union through the European Regional Development Fund – Competitiveness and Cohesion Operational Programme (Grant KK.01.1.1.02.0016.).

## References

- B. H. Northrop, Y. R. Zheng, K. W. Chi and P. J. Stang, *Acc. Chem. Res.*, 2009, **42**, 1554.
- G. R. Desiraju, *Crystal Engineering: The Design of Organic Solids*, Elsevier, Amsterdam, 1989.
- B. Moulton and M. J. Zaworotko, *Chem. Rev.*, 2001, **101**, 1629.
- M. J. Zaworotko, *Cryst. Growth Des.*, 2007, **7**, 4.
- B. Li, Q. Lei, T. Qin, X. Zhang, D. Zhao, F. Wang, W. Li, Z. Zhang and L. Fan, *CrystEngComm*, 2021, **23**, 8260.
- D. Kim, G. Kim, J. Han and O.-S. Jung, *Bull. Korean Chem. Soc.*, 2022, **1**.
- A. L. Gillon, N. Feeder, R. J. Davey and R. Storey, *Cryst. Growth Des.*, 2003, **3**, 663.
- M. Đaković, D. Vila-Viçosa, M. J. Calhorda and Z. Popović, *CrystEngComm*, 2011, **13**, 5863.
- A. Kobayashi, H. Konno, K. Sakamodo, A. Sekine, Y. Obashi, M. Iida and O. Ishitani, *Chem. – Eur. J.*, 2005, **11**, 4219.
- J. Moncol, M. Mudra, P. Lonneck, M. Hewitt, M. Valko, H. Morris, J. Svorec, M. Melnik, M. Mazur and M. Koman, *Inorg. Chim. Acta*, 2007, **360**, 3213.
- Z.-X. Lian, J. Cai, C.-H. Chen and H.-B. Luo, *CrystEngComm*, 2007, **9**, 319.
- B. R. Bhogala, P. K. Thallapally and A. Nangia, *Cryst. Growth Des.*, 2004, **4**, 215.
- M. H. Chou, D. J. Szalda, C. Creutz and N. Sutin, *Inorg. Chem.*, 1994, **33**, 1674.
- K. Sakai, M. Shiomi, T. Tsubomura, K. Kato, Y. Yokoyama, T. Kajiwara and T. Ito, *Acta Crystallogr., Sect. E: Struct. Rep. Online*, 2003, **59**, m559.
- H. Zhang, X. Wang, K. Zhang and B. K. Teo, *Coord. Chem. Rev.*, 1999, **183**, 157.
- R. G. Pearson, *J. Am. Chem. Soc.*, 1963, **85**, 3533.
- M. Kabešová, R. Boča, M. Melník, D. Valigura and M. Dunaj-Jurčo, *Coord. Chem. Rev.*, 1995, **140**, 115.
- M. Đaković, Z. Jagličić, B. Kozlevčar and Z. Popović, *Polyhedron*, 2010, **29**, 1910.
- Z. Popović and M. Đaković, *The structural features of metal pseudohalide complexes with pyridinecarboxamides, Nuclear magnetic resonance in chemistry, physics and biological sciences*, Plenary lecture, Book of abstracts, Warsaw, 2008, p. L17.
- M. Đaković and Z. Popović, *Acta Crystallogr., Sect. C: Cryst. Struct. Commun.*, 2009, **65**, m361.
- T. Neumann, I. Jess and C. Näther, *Acta Crystallogr., Sect. E: Crystall. Commun.*, 2016, **72**, 1077.
- T. Neumann, I. Jess and C. Näther, *Acta Crystallogr., Sect. E: Crystall. Commun.*, 2016, **72**, 1263.
- M. M. Wicht, L. R. Nassimbeni and N. B. Báthori, *Polyhedron*, 2019, **163**, 7.
- Oryx 8, Protein Crystallization Robot for Sitting Drop, Microbatch Screening and Optimization, Douglas Instruments, 2022.
- (a) CrysAlisPro Software System, *Version 1.171.38.41*; Rigaku Oxford Diffraction, 2015; (b) CrysAlisPro Software System, *Version 1.171.41.92a*, Rigaku Oxford Diffraction, 2020.
- G. M. Sheldrick, *Acta Crystallogr., Sect. A: Found. Adv.*, 2015, **71**, 3.
- O. V. Dolomanov, L. J. Bourhis, R. J. Gildea, J. A. K. Howard and H. Puschmann, *J. Appl. Crystallogr.*, 2009, **42**, 339.
- G. M. Sheldrick, *Acta Crystallogr., Sect. C: Struct. Chem.*, 2015, **71**, 3.
- A. L. Spek, *J. Appl. Crystallogr.*, 2003, **36**, 7.
- A. L. Spek, *Acta Crystallogr., Sect. D: Biol. Crystallogr.*, 2009, **65**, 148.
- L. J. Farrugia, *J. Appl. Crystallogr.*, 2012, **45**, 849.
- C. F. Macrae, I. J. Bruno, J. A. Chisholm, P. R. Edgington, P. McCabe, E. Pidcock, L. Rodriguez-Monge, R. Taylor, J. van de Streek and P. A. Wood, *J. Appl. Crystallogr.*, 2008, **41**, 466.
- K. Momma and F. Izumi, *J. Appl. Crystallogr.*, 2011, **44**, 1272.
- T. Degen, M. Sadki, E. Bron, U. König and G. Nénert, *Powder Diffr.*, 2014, **29**(S2), S13.
- J. D. Chai and M. Head-Gordon, *Phys. Chem. Chem. Phys.*, 2008, **10**, 6615.
- L. Hok, E. L. Sanchez, R. Vianello, B.-M. Kukovec and Z. Popović, *Eur. J. Inorg. Chem.*, 2021, **15**, 1470.

- 37 S. Roca, L. Hok, R. Vianello, M. Borovina, M. Đaković, L. J. Karanović, D. Vikić-Topić and Z. Popović, *CrystEngComm*, 2020, **22**, 7962.
- 38 N. Pantalon Juraj, G. I. Miletić, B. Perić, Z. Popović, N. Smrečki, R. Vianello and S. I. Kirin, *Inorg. Chem.*, 2019, **58**, 16445.
- 39 J. P. Foster and F. Weinhold, *J. Am. Chem. Soc.*, 1980, **102**, 7211.
- 40 M. J. Frisch, G. W. Trucks, H. B. Schlegel, G. E. Scuseria, M. A. Robb, J. R. Cheeseman, G. Scalmani, V. Barone, G. A. Petersson, H. Nakatsuji, X. Li, M. Caricato, A. V. Marenich, J. Bloino, B. G. Janesko, R. Gomperts, B. Mennucci, H. P. Hratchian, J. V. Ortiz, A. F. Izmaylov, J. L. Sonnenberg, D. Williams-Young, F. Ding, F. Lipparini, F. Egidi, J. Goings, B. Peng, A. Petrone, T. Henderson, D. Ranasinghe, V. G. Zakrzewski, J. Gao, N. Rega, G. Zheng, W. Liang, M. Hada, M. Ehara, K. Toyota, R. Fukuda, J. Hasegawa, M. Ishida, T. Nakajima, Y. Honda, O. Kitao, H. Nakai, T. Vreven, K. Throssell, J. A. Montgomery, Jr., J. E. Peralta, F. Ogliaro, M. J. Bearpark, J. J. Heyd, E. N. Brothers, K. N. Kudin, V. N. Staroverov, T. A. Keith, R. Kobayashi, J. Normand, K. Raghavachari, A. P. Rendell, J. C. Burant, S. S. Iyengar, J. Tomasi, M. Cossi, J. M. Millam, M. Klene, C. Adamo, R. Cammi, J. W. Ochterski, R. L. Martin, K. Morokuma, O. Farkas, J. B. Foresman and D. J. Fox, *Gaussian 16 (Revision C.01)*, Gaussian Inc., Wallingford, CT, 2016.
- 41 P. R. Spackman, M. J. Turner, J. J. McKinnon, S. K. Wolff, D. J. Grimwood, D. Jayatilaka and M. A. Spackman, *J. Appl. Crystallogr.*, 2021, **54**, 1006.
- 42 Q. Yin, E. V. Alexandrov, D.-H. Si, Q.-Q. Huang, Z.-B. Fang, Y. Zhang, A.-A. Zhang, W.-K. Qin, Y.-L. Li, T.-F. Liu and D. M. Proserpio, *Angew. Chem.*, 2022, **61**, e202115854.
- 43 G. Mahmoudi, M. Kubicki, D. Choquesillo-Lazarte, B. Mirosław, E. V. Alexandrov, P. N. Zolotarev, A. Frontera and D. A. Safin, *Polyhedron*, 2020, **190**, 114776.
- 44 C. Belle, C. Bougault, M.-T. Averbuch, A. Durif, J.-L. Pierre, J.-M. Latour and L. Le Pape, *J. Am. Chem. Soc.*, 2001, **123**, 8053.
- 45 R. Bala, R. P. Sharma, R. Sharma and B. M. Kariuki, *Inorg. Chem. Commun.*, 2006, **9**, 852.
- 46 R. Kapoor, A. Kataria, A. Panthak, P. Venugoplan, G. Hundal and P. Kapoor, *Polyhedron*, 2005, **24**, 1221.
- 47 V. H. M. da Silva, J. W. de Mesquita Carneiro, L. M. da Costa and G. B. Ferreira, *J. Mol. Model.*, 2020, **26**, 146.